Cooperative progression of colitis and leukemia modulated by clonal hematopoiesis via PTX3/IL-1β pro-inflammatory signaling

Hang He[1,2], Yuchen Wen[1,2], Hanzhi Yu[1,2], Jingjing Liu[1,2], Qingran Huo[1,2], Wenyan Jin[1,2], Zhiqin Wang[1,2], Guohui Du[3], Jun Du[4], Huaquan Wang[5], Zhigang Zhao[6], Zhigang Cai[1,2,4,5,*]

[1]The Province and Ministry Co-sponsored Collaborative Innovation Center for Medical Epigenetics; Department of Pharmacology, School of Basic Medical Science, Tianjin Medical University, Tianjin, China.
[2]National Key Laboratory of Blood Science, Tianjin, China.
[3]Department of Research and Development, Beijing SeekGene BioSciences Co. Ltd, Beijing, China.
[4]Department of Rheumatology and Immunology, Tianjin Medical University Tianjin General Hospital, Tianjin, China.
[5]Department of Hematology, Tianjin Medical University Tianjin General Hospital, Tianjin, China.
[6]Department of Medical Oncology, Tianjin First Central Hospital, School of Medicine, Nankai University, Tianjin, China.

[*]Correspondence:
Zhigang Cai, Professor, Ph.D.
Tianjin Medical University
No.22, Qixiangtai Road, Tianjin, China 200037
E-mail: US36zcai@tmu.edu.cn
Phone: (+86)18622633722

Abstract

Clonal hematopoiesis (CH) is suggested as an important risk factor for all-cause mortality and multiple chronic diseases including hematological neoplasms, cardiovascular diseases, and potentially a spectrum of autoimmune or immune-deficiency diseases. Mutations in *TET2* are one of the first identified, most important and prevalent genetic drivers of CH. However, cooperative factors and mechanisms underlying *TET2*-deficiency related CH (TedCH) remain largely unknown. Controversially, it is recently suggested that certain diseases take place prior to TedCH and promote TedCH on the contrary, indicating diseases in non-hematopoietic organs may act as environmental non-genetic drivers of CH. To clarify relationships between immune-dysfunctional diseases and CH, here we tested impact of various challenges on TedCH. We found that expedited TedCH depended on establishment of inflammatory environment. Primary or chimeric *Tet2*-mutant mice spontaneously developed co-symptoms reminiscent of human chronic colitis and myeloid leukemia, which was exacerbated by feeding with DSS, an experimental inducer of ulcerative colitis. Single cell RNA-seq (scRNA-seq) analysis reveals in depth the damage of colon and bone marrow in the *Tet2*-mutant mice in physiological condition or fed with DSS, along with increase of dysbacteriosis indicated by gut microbiome analysis. Results from colon scRNA-seq from both mouse and human highlight important roles of PTX3/IL-1β pro-inflammatory signaling in promoting colitis or leukemia. Finally, TedCH trajectory and inflammation in colon and bone marrow was ameliorated by treatment of IL-1R1 inhibitor Anakinra. Our study suggests that PTX3/IL-1β signaling and clonal hematopoiesis cooperates and plays important roles in gut-bone marrow axis and related diseases including colitis and leukemia.

Key words

Clonal hematopoiesis, colitis, leukemia, inflammation, *TET2, PTX3*, *IL-1β*, Anakinra

Highlights

1. Certain environmental factors such as Dextran Sulfate Sodium (DSS), an experimental inducer of ulcerative colitis, promotes *Tet2*-difficiency related clonal hematopoiesis (TedCH)

2. Colitis and leukemia are spontaneously and simultaneously developed in *Tet2*-defficient primary or chimeric mice, along with increased pathogenic gut microbiomes, indicating aberrant gut-bone marrow axis in the mutant mice.

3. Single cell RNA-seq analysis reveals enhanced PTX3, a soluble pattern recognition molecule (PRM) and IL-1β pro-inflammatory signaling in colitis and leukemia.

4. *In vivo* function of the PTX3/IL-1β pro-inflammatory signaling in TedCH is also indicated in human colitis and validated experimental settings.

Running Title

Colitis and Leukemia Co-modulated by PTX3/IL-1β Signaling and Clonal Hematopoiesis

Introduction

Clonal hematopoiesis (CH) is a phenomenon whereby hematopoietic stem cells (HSCs) carry genetic mutations with advantageous growth potential, resulting in aberrant expansion of certain immature and mature hematopoietic cell population over time (Genovese et al., 2014; Steensma et al., 2015). Similar phenomenon, somatic mutation-driven clonal expansion of certain cells, takes place in non-hematopoietic organs such as skin, esophagus, and brain (Jaiswal and Ebert, 2019). Recent studies suggest that CH is associated with an increased risk of developing hematological malignancies including acute myeloid leukemia (AML) and myelodysplastic syndrome (MDS). Scoring CH is able to stratify high-risk CH-carriers (Weeks et al., 2022). Interestingly, CH is also associated with non-hematological diseases including all-cause mortality, cardiovascular disease, chronic obstructive pulmonary disease, and gout (metabolic arthritis, an auto-immune disease in bone juncture) (Agrawal et al., 2022; Jaiswal and Libby, 2020; Jaiswal et al., 2017; Miller et al., 2022). Accordingly, World Health Organization recently recognizes that CH is a precursor lesion of myeloid neoplasms (Khoury et al., 2022). Therefore, characterizing drivers and consequences of CH will not only assist in investigating clonal expansion of somatic cells in non- hematopoietic organs but also help in understanding the etiology of numerous chronic diseases many years prior to their onset (Weeks et al., 2022).

Loss-of-function heterozygous mutations in the epigenetic regulator *TET2* (Ten-Eleven Translocation methyl-cytosine dioxygenase-2) were among the first discovered and one of the most prevalent and important drivers of CH. Unsurprisingly now, mutations in *TET2* are also the top prevalent single-gene mutations in MDS, an age-related hematological disease with abnormal hematopoietic stem and progenitor cells (HSPCs) (Delhommeau et al., 2009; Nazha et al., 2021). *Tet2*-deficient primary or chimeric mouse models display a competitive advantage over *Tet2*-deficient HSPCs, skewing myeloid differentiation, and a tendency to transform into full-blown leukemia when co-operative mutations and environmental factors involved in (e.g., $Flt3^{ITD/+}$ or $NRas^{G12D}$) (Moran-Crusio et al., 2011) (Cai et al., 2020a; Chu et al., 2012). Loss of *TET2* results in increase of DNA methylation at various genomic sites, such as promoters, enhancers, and CpG islands (Rasmussen et al., 2015). Recently we and others reported that *Tet2*-deficient HSPCs exhibit significantly increased expression of the inflammatory cytokine interleukin-6 (IL-6) and show stronger anti-apoptotic and self-renewal abilities after exposure to acute stimulus such as IL-6 or lipopolysaccharides (LPS), leading to the development of an age-dependent chronic myelomonocytic leukemia (CMML)-like disease in the mutant mice over time (Cai et al., 2018; Zhang et al., 2015). Microbial signals are a major source of inflammatory inducer and interestingly *Tet2* mutant mice with antibiotic treatment or raised in germ-free condition developed minimal CMML-like phenotypes (Meisel et al., 2018). In line with these studies, a most recent study based on *in vivo* models rather than generating chimeric *Tet2*-mutant models demonstrated that interleukin-1 (IL-1α and IL-1β), is able to act as an external factor in driving *Tet2*-deficiency related clonal hematopoiesis (TedCH) over age; genetic loss of their receptor *IL1-R1* mitigated *Tet2*-deficiency related abnormalities (Burns et al., 2022; Caiado et al., 2023). In summary, results from several independent studies strongly suggest that *Tet2*-deficient HSPCs manifest TedCH phenomenon and cooperate with intrinsic and extrinsic factors to develop stronger symptoms such as full-blown leukemia AML.

However, through mathematical analysis and experimental validation, a recent

study of TedCH suggests that hypercholesterolemia-induced atherosclerosis took place prior to clonal hematopoiesis and may act as a driver of *Tet2*-deficient HSCs proliferation on the contrary. This study suggests that certain diseases or environmental conditions, for example, atherosclerosis drives the onset and trajectory of TedCH (Heyde et al., 2021). Atherosclerosis is a complicated and chronic disease where inflammation dysregulation explains in part (if not all) the etiology: mononuclear cells from the blood, including white blood cells, are recruited to the vessel wall in response to tissue damage (Libby et al., 2002). To further demonstrate that "diseases" was able to take prior to TedCH and drive TedCH, the authors presented an additional experimental model, a sleep fragmentation model, and demonstrated that sleep disturbance drives TedCH (Heyde et al., 2021). Nonetheless, clarifying the drivers and consequences of TedCH is the most critical challenge in the area. Controlling the trajectory of TedCH will also assist in developing strategies to mitigate CH-related diseases.

In previous studies, we have identified LPS, an inducer of innate-immunity related TLR4 signaling, and mutations in *Flt3*, *Ins2* or lncRNA *Morrbid* cooperates with *Tet2* deficiency to exacerbate or mitigate TedCH or leukemic phenotypes(Cai et al., 2020a; Cai et al., 2018; Cai et al., 2021; Cai et al., 2020b). To extensively explore the potential drivers of CH, we further assessed the impact of another five different environmental factors on TedCH and confirmed that accelerated TedCH depends on the establishment of inflammatory environment. Based on the results of single cell RNA-seq in the organs of colon and bone marrow (mouse and human both included) and microbe sequencing in gut, we propose that PTX3/IL-1β signaling pathway, a tight complement/pro-inflammation cascade, play important roles in gut-bone marrow axis which in turn regulates clonal hematopoiesis. We suggest that the PTX3/IL-1β signaling should be appreciated to mitigate TedCH trajectory and related diseases including colitis and leukemia.

Results

DSS but not STZ, 5-FU, or additional irradiation promotes TedCH

Competitive bone marrow transplantation (cBMT) assays were developed for analyzing TedCH in the chimeric mice and four different treatments were chosen for testing environmental impacts on TedCH: DSS, STZ, 5-FU, and additional irradiation (**Figure 1A**). 5-FU and additional irradiation are well-known direct regulators of hematopoiesis while DSS induces colitis and systematic inflammation and STZ induces hypoglycemia. TedCH trajectory was monitored every 3 weeks by analyzing CD45.1, CD45.2 and CD45.1/CD45.2 chimerism in the peripheral blood (PB) of the chimeric mice. As shown in **Figure 1B** and **C**, expedited TedCH were observed upon DSS feeding compared to vehicle (Veh) feeding. Treatments with STZ or additional irradiation appear to have no effect on TedCH while 5-FU has significant inhibition on TedCH (**Figure 1D** to **F; Supplemental Figure 1A** to **C**). As DSS induces inflammation and colitis, we conclude that inflammation and colitis positively cooperate TedCH trajectory in the cBMT experimental setting.

DSS exacerbates colitis burden and aberrant dysbacteriosis in *Tet2*$^{+/-}$ primary mice

Since DSS expedited TedCH in the chimeric mice, we then asked in detail what are the in-middle biological and pathological processes and consequences during the

DSS challenge. We chose *Tet2*-defficient primary mice for further study since they are more stable and readily monitored in a large cohort without irradiation involvement (irradiation itself may damage gut histology). A previous report suggests that acute DSS challenge exacerbate inflammatory bowel disease (IBD) in *Tet2*-defficient primary (Zhang et al., 2015). We turned to ask about the impact of chronic colitis by three cycles of low-dose DSS feeding (**Figure 2A**). Consistently, even low-dose of DSS also induced exacerbated colitis in *Tet2*-defficient primary mice ($Tet2^{+/-}$_DSS vs. WT_DSS, **Figure 2B-E**). Upon DSS challenge, increased diseases score (based on colon H&E staining) were observed and confirmed by expression of gut barrier markers *Muc2* and *Occludin* (**Figure 2F** and **G**; and **Supplemental Figure 2A**). Interestingly, *Tet2*-defficient primary mice appear to develop colitis spontaneously as shown by FITC-D staining in the blood serum and H&E staining ($Tet2^{+/-}$_Veh vs. WT_Veh, **Figure 2H**; and **Supplemental Figure 2A**).

To ask to what extent *Tet2*-defficient primary mice manifest aberrant colon immunity, we performed 16S RNA sequence and compared the microbial composition between WT and *Tet2*-defficient primary mice ($Tet2^{+/-}$_Veh vs. WT_Veh), along with the comparison between WT and *Tet2*-defficient primary mice fed with DSS ($Tet2^{+/-}$_DSS vs. WT_DSS). Results of the microbial composition data calculated by principal component analysis (PCA) suggest the four groups distinguish each other very well (**Figure 2I**). Although the Simpson index of operational taxonomic units (OUT, measuring microbial community composition) level fails to distinguish the four groups (a higher Simpson index indicates lower community diversity, **Figure 2J**), the Chaos index of OUT level significantly distinguishes microbial communities of $Tet2^{+/-}$_Veh mice from that of WT_Veh mice (a higher Chaos index indicates higher community richness, **Figure 2K**). Upon DSS challenge, the Chaos index of OUT level in $Tet2^{+/-}$_DSS and WT_DSS were decreased compared to that in $Tet2^{+/-}$_Veh and WT_Veh, suggesting certain bacteria were dominant expanded. Further microbial analysis suggests that: (1) at phylum level, *Tet2*_DSS mice exhibited most increments in *Proteobacteria* and *Actinobacteria* (both are pathogenic and toxic to the animals, **Figure 2L**); (2) at genus level, different microbiome compositions are revealed for the comparison between $Tet2^{+/-}$_Veh and WT_Veh (**Figure 2M**). Detailed comparison between $Tet2^{+/-}$_Veh and WT_Veh or between $Tet2^{+/-}$_DSS and WT_DSS reveal that aberrant changes in microbial composition including probiotic microbials (circled by blue rectangles) or pathogenic microbials (circled by pink rectangles) (**Figure 2N** and **O;** and **Supplemental Figure 2B** and **C**). Analysis combining hematological parameters and microbial composition further confirm that the pathogenic microbial *Proteobacteria* are involved in alteration of Hemoglobin level and neutrophil percentage (**Supplemental Figure 2D** and **E**). Taken together, results from colon pathology and microbial 16S RNA sequencing suggest that without DSS feeding, *Tet2*-defficient primary mice have already manifest subtle colitis and aberrant microbial composition, especially increase of pathogenic microbials; upon DSS challenge, *Tet2*-defficient primary mice manifest exacerbated colitis and growth of pathogenic microbial in the colon tissue.

DSS induces aberrant hematopoiesis and skewed myelopoiesis, which are consistently revealed by flow cytometry and scRNA-seq analysis

To directly clarify the DSS effect on hematopoiesis, cells from blood, spleen and bone marrow were subjected to hematological cell counts, histology, and flow cytometry analysis. Consistently with our previous report that *Tet2*-defficient primary

mice manifest skewed myelopoiesis with or without LPS treatment (Cai et al., 2018), we observed similar trends in the *Tet2*-defficient primary mice compared to wild-type controls (**Supplemental Figure 3A** to **H**). As flow cytometry relies only on limited molecular markers but scRNA-seq transcriptomic assays can offer much more comprehensive landscape of various HSPCs, Lin$^-$ bone marrow cells from the 4 groups of animals were sorted for scRNA-seq analysis. After quality controls, around 5000 to 9000 cells
from each group were included in the further annotation analysis (**Figure 3A**). A total of 11 main populations including hematopoietic stem cells (HSC) and granucyte-monocyte progenitors (GMP-1, GMP-2, and GMP-3) are annotated and have relative different developmental hierarchies, indicated by the relative position in the plots of Uniform Manifold Approximation and Projection (UMAP). Cells that are very close to mature neutrophils, monocytes and B cells are also annotated and marked as neutrophil progenitors (NP), monocyte progenitors (MP) and progenitor of B cells (Pro_B). Each group has all of these 11 cellular populations and their compositions are quantified at percentage portion (**Figure 3B**). The expression of the annotation markers supports the developmental identify of the cells (**Figure 3C** and **D**; and **Supplemental Figure 4A**). Interestingly, in the one-by-one comparison, markers for HSCs (*Ifitm1*, *Egr*1 and *Nr4a1*) are upregulated in the comparison between *Tet2*$^{+/-}$_Veh vs. WT_Veh, or between *Tet2*$^{+/-}$_DSS vs. *Tet2*$^{+/-}$_Veh, or between WT_DSS vs. WT_Veh, or between *Tet2*$^{+/-}$_DSS vs. WT_DSS (HSCs genes are underlined in **Figure 3D** and **E**; and **Supplemental Figure 4B**). Analysis of differentially expressed genes (DEGs) reveals that stemness-related genes including *Egr1* are upregulated in the pools of HSC and GMP-1, as indicated in the scRNA-seq dataset in the comparison between *Tet2*$^{+/-}$_Veh vs. WT_Veh or between *Tet2*$^{+/-}$_DSS vs. WT_DSS (**Supplemental Figure 4C**). The heatmap of the top 50 signaling pathways in the pool of HSC and GMP-1 further indicate that inflammatory signaling pathways such as IL6-Jak-Stat3 signaling, inflammatory response, interferon alpha and grammar response are upregulated in the *Tet2*$^{+/-}$_Veh compared to WT_Veh; similar trends are observed in the *Tet2*$^{+/-}$_DSS compared to WT_DSS (**Supplemental Figure 4D** to **F**). Interestingly, we also observed that higher cell-cycle pathways take place in the HSC and GMP-1 of *Tet2*$^{+/-}$_Veh compared to WT_Veh, or in the HSC and GMP-1 of *Tet2*$^{+/-}$_DSS compared to WT_DSS (**Supplemental Figure 4D** to **F**). When numerous candidate marker genes that are critical for HSCs are considered, we found that the expression level of *Cd34* and *Il1r1* are increased (notice the max level of each panels of the four groups) and the their expression "region" are expanded (notice the circle in dashed-line) (**Figure 3G**), indicating pro-inflammatory IL1b signaling is involved in the HSCs of Tet2mut_Veh and the DSS-treated mice, compared to that of WT_Veh controls. RNA velocity analysis also suggest that the hematopoietic developmental trajectory is altered in Tet2_Veh or DSS treated mice compared to WT_Veh (**Figure 3H** and **Supplemental Figure 4G**) (Bergen et al., 2020; La Manno et al., 2018; Li et al., 2023). Taken together, scRNA-seq results revealed similar skewed myelopoiesis as shown by flow cytometry and also revealed alterations specific to the pools of HSC and GMP in the *Tet2*$^{+/-}$_Veh or *Tet2*$^{+/-}$_DSS mice compared to the respective controls.

scRNA-seq analysis of colon tissue highlights that cell-to-cell talk between *Ptx3*$^+$ fibroblasts and *Il-1β*$^+$ monocytes in promoting inflammation

Colon tissue from the 4 group of mice were also used for scRNA-seq analysis since this approach can provide a full-map of cell-to-cell talk at the single-cell resolution. After quality controls, around 3000 to 6000 cells from each group were

included in the further annotation analysis (**Figure 4A**). A total of 5 main populations including epithelial cells, stromal cells, and immune cells (myeloid cells, B cells, and T cells) are annotated in the UMAP plot for the first step (**Figure 4A**). Each group has these five main cell populations. However, *Tet2*$^{+/-}$_Veh, WT_DSS and *Tet2*$^{+/-}$_DSS appear to have a higher percentage of stromal cells compared to the WT_Veh control (**Figure 4B** and **C**). Expression density of the respective markers for the five main cell population is shown in **Figure 4D**. The overall enriched signaling pathway analysis suggests that inflammatory signaling pathway is upregulated in the myeloid cells of *Tet2*$^{+/-}$_Veh, WT_DSS and *Tet2*$^{+/-}$_DSS compared to the WT_Veh control (green rectangle, **Figure4E;** and **Supplemental Figure 5A**). Importantly, cell-cycle related pathway is also upregulated in the myeloid cells of *Tet2*$^{+/-}$_Veh compared to WT_Veh control (pink rectangle, **Figure4E**). Interestingly, we also observed upregulated epithelia-mesenchymal-transition pathway (EMT) in the stromal cells of *Tet2*$^{+/-}$_Veh, WT_DSS and *Tet2*$^{+/-}$_DSS compared to the WT_Veh control (blue rectangle, **Figure4E**; and **Supplemental Figure 5C**). Overall, the pathway enrichment analysis in each single cell population suggests that myeloid cells and stromal cells grossly have the most alterations in the comparison between *Tet2*$^{+/-}$_Veh vs. WT_Veh or between WT_DSS vs. WT_Veh. We then filtered out myeloid cells and stromal for further cell-to-cell talk analysis.

First, stromal cells and myeloid cells from the colon UMAP pool were subject to further clustering to distinguish sub-populations. In total, 8 sub-populations of cells in the stromal cells and 7 sub-populations of cells in the myeloid cells are annotated according to the typical marker gene expression (**Figure 4F;** and **Supplemental Figure 5B**). Expression of *Ptx3* and *Il-1β* are plotted in the UMAP space of colon tissue, stromal cells, or myeloid cells as indicated (**Figure 4G**). To our surprise, expression of *Ptx3* appears to be specific to stromal cells in the colon while expression of *Il-1β* appears to be specific to stromal cells in the colon in the scRNA-seq dataset.

Five sub-populations from the stromal cells and six sub-populations from the myeloid cells had the most alterations in the percentage and therefore were used for calculating cell-to-cell talk strength (**Figure 4H**). Indeed, *Cx3crl1*$^{+}$-myeloid cells appear to have stronger interaction with *Ptx3*$^{+}$-stromal cells in *Tet2*$^{+/-}$_Veh compared to WT_Veh (left two panels, **Figure 4H**). Myofibroblasts also appear to strongly interact with many myeloid cells in *Tet2*$^{+/-}$_Veh compared to WT_Veh (left two panels, **Figure 4H**). Upon DSS feeding, interaction between *Ptx3*$^{+}$-stromal cells and several myeloid cells are dramatically activated (right two panels, **Figure 4H**).

To dissect the detailed molecular events in the *Il-1β*$^{+}$-myeloid cells and *Ptx3*$^{+}$-stromal cells, five of myeloid sub-populations were used for NicheNet assay (Browaeys et al., 2020). As shown in **Figure 4I** to **L**, IL-1β/IL1-R1 signaling is actively involved in the cell-cell interaction, associated with expression of many downstream genes encoding complement protein proteins or inflammatory ligands (*C1ra*, *C1s1*, *C3* and *Cxcl12*). Surprisingly, *Il1r1* along with *C1ra*, *C1s1*, *C3* and *Cxcl12* all are dominantly expressed in the stromal cells of colon, compared with other four main cell population (**Supplemental Figure 5D**). Taken together, our detailed cell-cell talk analysis based on the colon scRNA-seq dataset from the 4 groups of mice strongly suggest that PTX3/IL-1β axis recruits inflammatory and complement cascade to module colon immunity in *Tet2*-deficient mice fed with DSS or raised in normal condition.

Aberrant expression of *PTX3* and *IL-1β* are indicated clinical samples with

leukemia or colitis.

To guarantee that PTX3/IL-1β signaling involves in human colitis or leukemia, we searched publicly available datasets of bulk RNA-seq or scRNA-seq and compared their expression between disease group and healthy controls. Data shown in **Figure 5A** to **D** suggest that increased expression of *PTX3* is detected in the myeloid leukemia group (datasets with AML or MDS patients were analyzed). Interestingly, mutations in *TET2* appear to have higher expression of *PTX3* also (**Figure 5A** and **D**). Importantly, higher expression of *PTX3* has a worse prognosis in the TCGA-LAML cohort while expression of *IL-1β* failed to stratify the cohort (**Figure 5A** and **D**). Additionally, analysis of colitis samples also suggests that higher expression of *PTX3* and *IL-1β* took place in some cohorts of colitis samples compared to the controls (**Figure 5E** to **G**). Taken together, these results warrant that the PTX3/IL-1β bundle indeed involves in human colitis or leukemia.

As we surprisingly observed that *Ptx3* and *Il-1r1* are dominantly (if not specifically) expressed stromal cells of colon tissue in mice (**Figure 4G** and **M;** and **Supplemental Figure 7A** and **B**), we want to characterize if this pattern is conserved in human. We downloaded the publicly available scRNA-seq datasets of colitis and re-analyzed the cells (Smillie et al., 2019). Results from **Figure 5H** to **M**, along with **Supplemental Figure 6,** suggest that the percentage of *PTX3*$^{+}$-fibroblasts indeed increased according to the grade of colitis. Although partial myeloid cells express *PTX3* themselves, *PTX3* is also dominantly expressed in stromal cells. Taken together, results from human clinical samples suggest that PTX3/IL-1β signaling may have important function in colitis and leukemia.

Pharmacological blockage of IL-1β signaling by Anakinra inhibits PTX3 expression and inflammation in colon and mitigates TedCH in blood

PTX3 is a soluble pattern recognition molecule (PRM) and has been reported to directly involves in IL-1β signaling (Bonavita et al., 2015). We postulate that the PTX3/IL-1β signaling pathway is present at the protein level in the colon of *Tet2*$^{+/-}$ mice with chronic inflammation. To validate this hypothesis, we performed western blot analysis to examine the expression of Il-1β and Ptx3 (**Supplemental Figure 7**C and **D**). Additionally, immunohistochemical (IHC) staining revealed high levels of Ptx3 expression in inflammatory cells infiltrating the colonic tissues of *Tet2*$^{+/-}$ mice (**Supplemental Figure 7E** and **F**).

As inhibitors specific to PTX3/Ptx3 activity are not available, we turn to use IL1R1 specific inhibitor Anakinra to assess the function of Ptx3 in the TedCH, colitis and aberrant hematopoiesis. cBMT assays for TedCH were conducted along with DSS and/or Anakinra treatment (**Figure 6A**). Consistent with its anti-inflammation function, application of Anakinra mitigate TedCH expansion in the mice feed with Vehicle or DSS (**Figure 6B;** and **Supplemental Figure 7G**). Aberrant hematopoiesis also appears to be partially rescued in the TedCH_Anakinra mice compared to TedCH_PBS mice (**Figure 6B;** and **Supplemental Figure 7H** and **K)**. Importantly, application of Anakinra reduced the expression of both Ptx3 and Il-1β (**Figure 6D** and **E**)**.** The reduced expression of Ptx3 upon Anakinra is also validated by immunohistochemistry (IHC) and pathologic index is largely ameliorated upon Anakinra treatment (**Figure 6F** to **I**). Taken together, results from Anakinra treatment suggest that inhibition of Il-1β signaling modulated Ptx3 expression and inflammation severity, along with TedCH trajectory and aberrant hematopoiesis.

Discussion

Since clonal hematopoiesis was for the first time recognized as a new risk medical entity to broadly predict diseases and even all-cause mortality around a decade ago, numerous genetic drivers or passengers of clonal hematopoiesis have been characterized, along with a recent report indicating their trajectories were able to be mathematically computed in human samples (Abelson et al., 2018; Fabre et al., 2022; Genovese et al., 2014; Weeks et al., 2022; Weinstock et al., 2023).To understand the mechanisms underlying CH, it was proposed that different genetic drivers of CH may favor corresponding environmental factors to strengthen or amplify the onset and consequence of CH (Caiado et al., 2021). For example, mutations in *TP53* and *PPM1D,* two top-10 prevalent drivers of CH, were selected when irradiation was applied in the therapy or after exposure to cisplatin and doxorubicin treatment (Wong et al., 2015) (Hsu et al., 2018). Our previous studies have shown that mutations in *TET2*, the first identified and one of the top-3 driver of CH, favors inflammatory condition on the contrary; blocking inflammation by genetic loss of *Morrbid* or administration of anti-inflammation drugs E3330 or SHP099 mitigate TedCH in experimental models (Cai et al., 2020a; Cai et al., 2018; Cai et al., 2021; Cai et al., 2020b). However, whether and how other environmental factors (positive, negative, or neutral to TedCH), intra-cell or intra-organ or host-pathogen communications drives TedCH remain incompletely understood.

To reach these aims, we first assessed the role of five different environmental factors in TedCH (4 factors are included in this study; and another one based on *Tet2*$^{+/-}$ HSPCs mixed with genetically stable inflammatory HSPCs will be reported elsewhere) and prioritized the impact of DSS, an inducer of infection with toxic pathogens and colitis in gut. We further characterized the impact of DSS on the *Tet2*-deficient chimeric or primary mice by multi-omic tools including single cell RNA sequencing or gut microbe sequencing. Although administration of the other three challenges, irradiation, 5-FU (depletion of immune cells and hematopoietic cells), or STZ (toxic damager of pancreases and inducer of high blood glucose) failed to accelerate TedCH, chronic colitis induced by three cycles of feeding with DSS or mixing with IL-1β-secreting genetically stable inflammatory HSPCs expedite the trajectory of TedCH. These results suggest that: 1) only certain specific environmental factors play a positive role to cooperate with TedCH in experimental models; 2) these "positive" factors may have a direct link to inflammation or innate immunity; 3) an intra-organ communication, gut-bone marrow axis, which could be stimulated by host-pathogen axis or just by dysregulated auto-immunity, play a role in TedCH and leukemogenesis.

These observations from us are consistent with a previous study by *Meisel* et al. who directly studied the pathogen-host interaction in *Tet2*-mutation mediated leukemic diseases. In the study, *Meisel* et al. systematically studied why *Tet2*-mutant primary mice did not develop MPN or CMML phenotypes with 100% penetration and proposed that microbial signals cooperate to induce pre-leukemic MPN phenotype in the mice (host-pathogen axis in TedCH-related diseases). Using *Tet2*-mutant mice raised in germ-free condition, the authors further solidly validate their conclusions (Meisel et al., 2018; Zeng et al., 2019). However, most of the experimental mice and our human are exposed to microbial environment during life. Where the initial inflammation take place (gut, bone marrow or even other organ?) and how it triggers CH and changes its trajectory remain to be elucidated.

Considering the importance of inflammation in *Tet2*-mutation related diseases, in previous studies we integrated multiplayers and proposed a working model for *Tet2*-

449 mutation related diseases: TedCH recruits a feed-forward loop and inflammation acts
450 as an amplifier in the loop for diseases progression including chronic leukemia and
451 acute leukemia (Cai et al., 2018; Cai et al., 2021). Given that DSS promotes TedCH in
452 chimeric mice, we then tested if DSS could promote *Tet2*-mediated CMML to
453 transform into full-blown AML. During the short-period of colitis, we indeed notices
454 exacerbated phenotypes in *Tet2*mutant_DSS mice in both gut permeability (worsen
455 colitis) and bone marrow hematopoiesis (malignant transformation to MDS/MPN-
456 like). Unlike that we observed full-blown AML in aged $Tet2^{+/-};Flt3^{ITD/ITD}$ or
457 $Tet2^{+/-};Ins2^{+/-}$, we failed to observe full-blown AML in the DSS-challenged mice.
458 These results suggest that inflammation as an amplifier to induce full-blown AML
459 may depend on adequate time.
460 Furthermore, single-cell RNA-seq (scRNA-seq) today becomes a very powerful
461 tool to dissect the etiology of complicated diseases at single cell level and molecular
462 level. Both scRNA-seq and bulk RNA-seq were applied in this study to delineate the
463 widespread transcriptional changes in bone marrow and gut (note that only lineage-
464 negative bone marrow cells were sorted for scRNA-seq analysis to prioritize
465 alterations in hematopoiesis). Consistent with previous studies, functional enrichment
466 analysis of DEGs in HSC and CMP showed that stem cell self-renewal and immune
467 responses related genes were upregulated in *Tet2*-deficient mice treated with DSS.
468 These observations were unlikely to be gained years ago since minimal HSC and
469 CMP cells could be sorted for RNA-seq and the sorted cells may not represent their
470 physiological conditions. Indeed, analysis of scRNA-seq in gut of *Tet2*-mutant_veh
471 and *Tet2*-mutant_DSS mice helps us to reveale a previously unappreciated alteration
472 in $Ptx3^{+}$-fibroblast of gut and the inferred PTX3/IL-1β signaling [note that mice were
473 raised in specific pathogen-free (SPF) condition with or without feeding with DSS].
474 These results make us conclude that *Tet2*-mutant mice appear to develop colitis and
475 leukemia simultaneously, very subtle if not strong, reminiscent of human symptoms.
476 Consistently, the involvement of PTX3/IL-1β inflammatory signaling is also
477 confirmed when we re-analyzed human colitis scRNA datasets.
478 Recent studies report that patients with inflammatory bowel disease (IBD) are
479 associated with clonal hematopoiesis and mutations in *DNMT3A* and *PPM1D* are
480 prevalent although mutations in *TET2* is not dominant in the cohort on the contrary
481 (Zhang et al., 2019). The colitis patients harbor mutant hematopoietic clones and
482 often present with clinical symptoms of MDS/AML (Cumbo et al., 2022). Moreover,
483 intestinal barrier dysfunction is also reported at diagnosis in patients with MDS and
484 AML (Khan et al., 2021). Along with these clinical observations, we conclude that
485 *Tet2*-mutant mice manifest co-symptoms of colitis and leukemia and that a molecular
486 link, PTX3/IL-1β signaling, may modulate both diseases in the mice.
487 Changes in the gut microbiome are considered a key regulator of the conversion of
488 normal hematopoiesis to diseased hematopoiesis, such as anemia and neutropenia
489 caused by IBD or long-term antibiotic use (Deshmukh et al., 2014). A study has
490 shown that an imbalance in the microbiota induced by antibiotic exposure or sterile
491 conditions can lead to dysregulation of hematopoiesis (Yan et al., 2018). Our data
492 from 16S rRNA gene sequencing indicated that $Tet2^{+/-}$ mice had disturbed gut
493 microbiota with significantly reduced probiotic abundance prior to the addition of
494 inflammatory factors. For example, chronically infected $Tet2^{+/-}$ mice exhibited
495 increased *Proteobacteria* and *Actinobacteria*, two toxic gut pathogens to mammals.
496 We also observed that there was a positive correlation between these microbiotas and
497 PB hematological parameters (**Supplemental Figure 2E**). Previous clinical studies
498 have shown that patients undergoing hematopoietic stem cell transplantation (HSCT)

have reduced gut microbiota diversity and increased *Proteobacteria*, which correlates with the risk of patients developing bloodstream infections during HSCT (Taur et al., 2012). These results suggest a potential role of microbial signaling in exacerbating the disease burden of IBD in *Tet2*$^{+/-}$ mice as well as hematologic malignancy transformation. Functional analysis in the appropriate facility with adequate biological protection, for example pathogen infection or fecal microbial transplantation, will offer direct evidence with regards the interaction between specific-pathogens and TedCH or *Tet2*-mutant mice (Zeng et al., 2023).

Consistent with previous studies (Burns et al., 2022; Caiado et al., 2023), in the context of DSS challenged-TedCH, our data suggest that anakinra eliminates the *Tet2*$^{+/-}$ clones in the clonal expansion in neutrophil and HSPC compartments, inhibits gut inflammation, and restores the adaptive hematopoietic injury induced by chronic inflammation. However, it does not fully restore the established clonal dominance in the HSPC pool, which may be partially addressed by increasing the treatment dose and duration. Dissecting the role in a cell-type specific deletion will assist in further understanding the cellular communications, i.e., immune cells with epithelia cells and offer a new knowledge for understanding gut-bone marrow axis and co-symptoms of colitis and leukemia. Based on our pharmacological data using the IL-1R inhibitor Anakinra, it is feasible to speculate that: 1) cocktails of antibiotics administration would also be able to slowdown TedCH, which should be tested in future studies; 2) blocking the IL-1β/PTX3 axis may represent a promising therapeutic target for preventing and treating infection-related clonal hematopoiesis and associated diseases. Since specific PTX3 inhibitors, except PTX3 antibodies, are still not available in research-grade or clinical-grade, developing PTX3 inhibitors or combining them with methylation drugs may represent potential therapeutic approaches for targeting *TET2* mutant hematopoiesis in the future.

In summary, the present study demonstrates that gut-bone marrow axis plays an important role in the co-symptoms of colitis and leukemia in the *Tet2*-mutant chimeric and primary mice. Dysbacteriosis, chronic inflammation and clonal hematopoiesis are all assembled to promote the progression the co-symptoms over age. Our single-cell transcriptomic analysis highlights and appreciates the role of a population of gut *Ptx3*$^{+}$-fibroblasts in driving the entire diseases. Mitigation of inflammation by IL-1R1 inhibitor Anakinra can downregulate Ptx3, repair gut barrier and slowdown TedCH. The study therefore demonstrates that PTX3/IL-1β signaling-associated clonal hematopoiesis plays important roles in gut-bone marrow axis and related chronic diseases including colitis and leukemia.

Materials and Methods

Materials and Methods including mice breeding, experimental procedures, mouse disease scoring and histology, computational analysis of single-cell RNA-seq and gut microbiome sequencing, collection, and analysis of clinical RNA-seq datasets, and statistical analysis are provided in detail in the **Supplemental File-1**. Computational environments with Linux and R language for analyzing scRNA-seq data and gut microbiome sequencing data have been described in our previous study (He et al., 2022). Custom scripts for analyzing and visualizing the omics results are available upon reasonable request.

Conflict of Interest

The authors declare that the research was conducted in the absence of any commercial

or financial relationships that could be construed as no potential conflict of interest.

Author Contributions

ZC and HH conceived and designed the study, wrote the computational scripts for sequencing analysis, visualized the results, drafted, and wrote the manuscript. HH performed most of the experiments and analysis. YW, HY, QH, WJ, ZW and JD assisted the experimental verification or validations from other database/cohorts and edited the manuscript. HW and ZZ contributed critical reagents and analyzed the data. All authors contributed to the editing and revision of the manuscript.

Funding

This work was supported in part by grants from the Tianjin Medical University Talent Program and from National Science Foundation of China to ZC (No.82170173).

Acknowledgments

We thank members of Cai laboratory and colleagues of Tianjin Medical University for their technical and administration support, critics and helpful suggestions improve the manuscript. We would also thank Drs. Mingjiang Xu, Tao Cheng, Hui Cheng, Zhiqiang Liu for sharing us reagents.

Figure Legends:

Figure 1. Assessing impacts of various treatments on TedCH trajectory.

(A) Competitive bone marrow transplantation (cBMT) assays were used for searching cooperative environmental factors of TedCH. See Methods for detailed cBMT experimental procedures. Treatments were applied once TedCH is set up at the 4~6 weeks post cBMT. Results of four different treatments (DSS, STZ, 5-FU and additional irradiation) were included in this study. As shown in the Figure 1A, DSS expedited TedCH. Expedited TedCH was also observed when *Tet2*$^{+/-}$ HSPCs were mixed with genetically stable inflammatory HSPCs and the detail results will be reported in another study (Wen and Cai *et al*., manuscript in preparation, 2023). cBMT, competitive bone marrow transplantation; PB, peripheral blood.

(B and C) Representative flow profiles of PB from the chimeric mice feed with DSS or normal water (vehicle, veh) (B) and the quantified trajectories of TedCH in the chimeric mice (C).

(D-F) Quantified trajectories of TedCH in the chimeric mice treated with STZ (D), or 5-FU (E), or additional irradiation (F) as indicated.

Data are shown as means ± SEMs. Number of biological repeats (animals): n = 5~7. Experiment of DSS treatment were repeated twice. Experiments of STZ or 5-FU or additional irradiation treatment were performed once.*, $p < 0.05$; **, $p < 0.01$; ***, $p < 0.001$; ****, $p < 0.0001$.

See also **Supplemental Figure 1** for representative flow profiles of PB from the chimeric mice with or without STZ, 5-FU and additional irradiation treatment.

Figure 2. *Tet2*-deficient mice manifest exacerbated colitis and aberrant microbiota composition when fed with DSS or vehicle.

(A) Experimental scheme for induction of chronic colitis by DSS. Three cycles of DSS feeding were performed during the 50-day experimental procedure. Four groups of animals were included in the entire procedure: WT_Veh, *Tet2*$^{+/-}$_Veh, WT_DSS, *Tet2*$^{+/-}$_DSS.

(B and C) Body weights and disease scores (disease activity index, DAI) were monitored daily and plotted during the induction.

(D-F) *Tet2*-deficient mice manifest exacerbated colitis based on colon pathology. Colons from the 4 groups of mice were photographed (D) and quantified based on colon length (E). Damage scores of colons were monitored and plotted based on H&E staining (F).
(G) Expression of two classic gut barrier markers *Muc2* and *Occludin* in colon were quantified by qRT-PCR.
(H) Damage of gut barrier were quantified by FITC-dextran staining in serum of PB.
(I-N) Microbiota (16S rRNA) sequencing analysis of gut in mice feed with DSS or vehicle. The PCA plot of the 4 groups of microbiota samples suggests obvious separation in microbial composition (I). α-diversity of the microbial community based on observed operational taxonomic units were quantified by Simpson or Chao index (J and K). Average relative abundance of prevalent microbiota at the phylum level or at the genus level among the four groups (L and M). Detailed comparison of relative taxon abundance between the *Tet2*$^{+/-}$*_Veh* vs. *WT_Veh* or between *Tet2*$^{+/-}$*_DSS* vs. *WT_DSS* are also shown in (N) and (O).
PCA, principal component analysis.
Data are shown as means ± SEMs in A to H. Number of biological repeats (animals): n = 3~7. Experiments of DSS treatment on primary mice were repeated three times. *, $p < 0.05$; **, $p < 0.01$; ***, $p < 0.001$; ****, $p < 0.0001$.
See also **Supplemental Figure 2** for representative photography of H&E staining of colons and additional microbiota analysis.

Figure 3. Single-cell RNA-seq analysis of HSPCs from *Tet2*-deficient mice when feed with DSS or vehicle.
(A) UMAP plot showing 11 main populations in Lin$^-$ BM cells. A total of 26,341 high-quality cells with an average of about 3000 genes per cell were included in the UMAP plot. After quality control during the dataset analysis, the group of *WT_Veh* has 7267 cells; *Tet2mut_Veh* has 4793 cells. *WT_DSS* has 5270 cells; *Tet2mut_DSS* has 9011cells. 1, HSC: hematopoietic stem cell; 2, CLP: common lymphoid progenitor; 3, GMP-1: granulocyte-macrophage progenitor-1, which may be close to CMP (common myeloid progenitor) in flow cytometry; 4, GMP-3: granulocyte-macrophage progenitor; 5, MMEP: mast and megakaryocyte-erythroid progenitor; 6, GMP-2: granulocyte-macrophage progenitor-2, which may be close to monocyte-dendrite progenitor; 7, MP: monocyte progenitor; 8, MkP: megakaryocyte progenitor; 9, NP: neutrophil progenitors; 10, ErP: erythroid progenitor; 11, Pro_B: progenitor of B cell.
(B) Stacking bar plot showing the portion of the 11 main annotated populations in each Lin$^-$ BM cell sample.
(C and D) Representative annotation markers of the 11 main cell populations in the scRNA-seq analysis of Lin$^-$ BM cell. In C, expression of *Flt3*, *Cebpe*, *Il6ra* and *Spi1* are highlighted in WT_Veh dataset. In D, each cell population has 4 typical markers in the dot plots.
(E) Top 20 DEGs (10 up-regulated and 10 down-regulated) are showed in each comparison when average expression of genes is calculated in each sample.
(F and G) Expression level and region of *Cd34* and *Il1r1* in the 4 group of scRNA-seq datasets.
(H) Hematopoietic cell trajectory inferred by RNA velocity with 24 selected critical genes, which are with known function in hematopoiesis. Notice the abnormal trajectory in NP and MP region, compared to WT_Veh.
DEG, differential expressed gene. UMAP, uniform manifold approximation and

projection.
See also **Supplemental Figure 3 and 4** for flow cytometry results and additional analysis of scRNA-seq Lin$^-$ BM dataset.

Figure 4. Single-cell RNA-seq analysis of colon tissue from *Tet2*-deficient mice when feed with DSS or vehicle.

(A) UMAP plot showing 5 main populations in colon tissues. After lysis of colon tissue, all cells from the colon tissue were subjected for scRNA-seq. A total of 18,092 high-quality cells with an average of about 3000 genes per cell were included in the UMAP plot. After quality control during the dataset analysis, the group of *WT_Veh* has 5589 cells; *Tet2mut_Veh* has 5649 cells; *WT_DSS* has 3382 cells; *Tet2mut_DSS* has 4372 cells. The 5 main populations include epithelial cells (red), stromal cells (yellow) and three major types of immune cells: myeloid cells (green), B cells (blue) and T cells (dark blue).

(B) Four individual UMAP plots are separately showed according to the sample source.

(C) Stacking bar plot showing the portion of the 5 main annotated populations in each colon sample.

(D) Expression of representative annotation markers for the 5 main cell populations in the UMAP plot of colons. *Dcn* for stromal cells; *Krt*8 for epithelial cells; *Lyz2* for myeloid cells; *Igha* for B cells; and *Trbc2* for T cells.

(E) Heatmap of dysregulated biological pathways in the 5 populations of colon tissues from 4 groups of samples. A full version of the heatmap is showed in the **Supplemental Figure 5**. Of note, Il6-Jak-Stat3 signaling, inflammatory response and interferon alpha response are upregulated in *Tet2mut_Veh, WT_DSS, and Tet2mut_DSS* in myeloid cell, compared to *WT_Veh* (circled by green rectangle). Additionally, proliferation-related pathways appear to be upregulated in myeloid cells of *Tet2mut_Veh* compared to *WT_Veh;* proliferation-related pathways appears to upregulated in T cells of *WT_DSS* and *Tet2mut_DSS* compared to *WT_Veh* (circled by pink rectangle). Interestingly, the epithelial mesenchymal transitional (EMT) pathway appears to be dysregulated in *Tet2mut_Veh, WT_DSS,* and *Tet2mut_DSS* in myeloid cell, compared to *WT_Veh* (circled by blue rectangle).

(F) Stromal cells and myeloid cells are subjected for further clustering by UMAP as they have most significantly upregulated biological pathways as indicated in (E). Top panel, UMAP plot of stromal cells and stacking plot showing potion of the sub-population; bottom panel, UMAP plot of myeloid cells and stacking plot showing potion of the sub-population. As indicated, 10 subpopulations and 7 subpopulations are annotated in stromal cells and myeloid cells respectively.

(G) Expression of *Ptx3* and *Il-1β* in the colon tissues (left panel) or in stromal cells (up-right panel) or in myeloid cells (bottom-right panel), respectively.

(H) Heatmap of cell-to-cell talk strength between subpopulations of stromal cells and myeloid cells.

(I-L) Detailed molecular events of the cell-to-cell talk between myeloid cells and stromal cells. Of note, *Ptx3*$^+$ fibroblasts and *Il-1β*$^+$ monocytes appear to be most involved. *Il-1β*$^+$ monocytes express numerous ligands including *Il-1β* (I and J). *Il-1β* binds *Il-1r1* in *Ptx3*$^+$ fibroblasts and stimulate a couple of downstream genes (K and L).

(M) Expression of *Il-1β* receptor *Il1r1* and relevant genes encoding complement components or inflammation regulators (*C1ra*, *C1s1*, *C3* and *Cxcl12*) were plotted on UMAP of colon tissue (top panel) or on the UMAP plot of stromal cells (bottom

panel).
See also **Supplemental Figure 5** for additional analysis of scRNA-seq colon dataset.

Figure 5. Aberrant PTX3/IL-1β signaling is indicated in human leukemia or colitis through analysis of clinical samples.
(A) Expression of *PTX3* and *IL-1β* in unsorted AML patients (left panel) or in AML patients carrying *TET2* mutation (right panel). Bulk RNA-seq datasets of bone marrow were included in the analysis.
(B-C) Prognosis value of marker genes *PTX3* and *IL-1β* in the TCGA-LAML cohort.
(D) Expression of *PTX3* and *IL-1β* in unsorted MDS patients (left panel, bone marrow samples) or in MDS patients carrying *TET2* mutation (right panel, bone marrow samples).
(E-G) Expression of *PTX3* and *IL-1β* in patients with ulcerative colitis and healthy controls, based on three independent cohorts. Bulk RNA-seq datasets of colon tissues were included in E and F; Bulk RNA-seq dataset of blood were included in G.
(H-L) Aberrant expression of *PTX3* and *IL-1β* was also detected using scRNA-seq dataset of human colitis samples. The dataset is downloaded from the website Broad Data Use Oversight System (https://duos.broadinstitute.org) and re-analyzed. The cohorts include two groups of human colon samples: colons from healthy controls (n=10) and colons from ulcerative colitis patients (n=7). Patient samples from both non-inflamed region and inflamed region were n=7 respectively. Inflammation scores suggesting the three group has significant difference overall (H). UMAP plots of the human colon scRNA-seq dataset also show five main population as similar as Figure 4A: epithelia cells, stromal cells and three immune cells (myeloid cells, B cells and T cells) (I). Stromal cells were highlighted by the dotted lines (I). Stromal cells were further annotated by UMAP plots and *PTX3*$^{+}$ fibroblasts were screened out by dotted lines (J). Of note, stacking plots indicate percentage of *PTX3*$^{+}$ fibroblasts were increased according the inflammation grade of the colitis (K). Expression of *PTX3* is shown in the UMAP plot of colon tissue (L) and three groups of stromal cells (M) as indicated.
See also **Supplemental Figure 6** for additional analysis of human colitis scRNA-seq dataset.

Figure 6. Pharmacological blockage of Il-1β signaling by Anakinra inhibits Ptx3 expression and inflammation in colon and mitigates TedCH in blood.
(A) Schematic representation of Anakinra treatment on the DSS-induced expedited TedCH.
(B) Quantification of PB chimerism in TedCH mice treated with DSS and/or Anakinra.
(C) Quantification of HSPCs including LSK, HSC, MPP2, MPP3/4, CMP and GMP in 4 groups of TedCH mice.
(D-E) The proteins level of Il-1β and Ptx3 were measured in colon tissues and quantified.
(F-G) Representative H&E staining of colon tissue from each group and diseases score (damages in colon tissue) were quantified accordingly. Scale bar is 500 μm.
(H-I) Representative immunohistochemical (IHC) staining of Ptx3 in colon (H) and semi-quantitative analysis of immunohistochemistry staining of Ptx3 based on integrated optical density (IOD) (I). scale bar is 100 μm.
Data are shown as means ± SEMs in A-H. Number of biological repeats (animal mouse): n = 5~7. Experiments of DSS treatment combining with Anakina on TedCH

mice were repeated twice. *, $p < 0.05$; **, $p < 0.01$; ***, $p < 0.001$; ****, $p < 0.0001$. See also **Supplemental Figure 7** for additional analysis of Ptx3 expression in TedCH colons.

Figure 7. Schematic illustration for the working model about clonal hematopoiesis cooperating with inflammation and dysbacteriosis in gut-bone marrow axis to promote colitis and leukemia.
We propose that gut-bone marrow axis plays important role in the co-symptoms of colitis and leukemia in the *Tet2*-mutant chimeric and primary mice. Dysbacteriosis, chronic inflammation and clonal hematopoiesis are all assembled to promote the progression the co-symptoms over age. See the main text for further discussion.

References

Abelson, S., Collord, G., Ng, S.W.K., Weissbrod, O., Mendelson Cohen, N., Niemeyer, E., Barda, N., Zuzarte, P.C., Heisler, L., Sundaravadanam, Y., *et al.* (2018). Prediction of acute myeloid leukaemia risk in healthy individuals. Nature *559*, 400-404.

Agrawal, M., Niroula, A., Cunin, P., McConkey, M., Shkolnik, V., Kim, P.G., Wong, W.J., Weeks, L.D., Lin, A.E., Miller, P.G., *et al.* (2022). TET2-mutant clonal hematopoiesis and risk of gout. Blood *140*, 1094-1103.

Bergen, V., Lange, M., Peidli, S., Wolf, F.A., and Theis, F.J. (2020). Generalizing RNA velocity to transient cell states through dynamical modeling. Nature Biotechnology *38*, 1408-1414.

Bonavita, E., Gentile, S., Rubino, M., Maina, V., Papait, R., Kunderfranco, P., Greco, C., Feruglio, F., Molgora, M., Laface, I., *et al.* (2015). PTX3 is an extrinsic oncosuppressor regulating complement-dependent inflammation in cancer. Cell *160*, 700-714.

Browaeys, R., Saelens, W., and Saeys, Y. (2020). NicheNet: modeling intercellular communication by linking ligands to target genes. Nat Methods *17*, 159-162.

Burns, S.S., Kumar, R., Pasupuleti, S.K., So, K., Zhang, C., and Kapur, R. (2022). Il-1r1 drives leukemogenesis induced by Tet2 loss. Leukemia *36*, 2531-2534.

Cai, Z., Aguilera, F., Ramdas, B., Daulatabad, S.V., Srivastava, R., Kotzin, J.J., Carroll, M., Wertheim, G., Williams, A., Janga, S.C., *et al.* (2020a). Targeting Bim via a lncRNA Morrbid Regulates the Survival of Preleukemic and Leukemic Cells. Cell Rep *31*, 107816.

Cai, Z., Kotzin, J.J., Ramdas, B., Chen, S., Nelanuthala, S., Palam, L.R., Pandey, R., Mali, R.S., Liu, Y., Kelley, M.R., *et al.* (2018). Inhibition of Inflammatory Signaling in Tet2 Mutant Preleukemic Cells Mitigates Stress-Induced Abnormalities and Clonal Hematopoiesis. Cell Stem Cell *23*, 833-849.e835.

Cai, Z., Lu, X., Zhang, C., Nelanuthala, S., Aguilera, F., Hadley, A., Ramdas, B., Fang, F., Nephew, K., Kotzin, J.J., *et al.* (2021). Hyperglycemia cooperates with Tet2 heterozygosity to induce leukemia driven by proinflammatory cytokine-induced lncRNA Morrbid. J Clin Invest *131*.

Cai, Z., Zhang, C., Kotzin, J.J., Williams, A., Henao-Mejia, J., and Kapur, R. (2020b). Role of lncRNA Morrbid in PTPN11(Shp2)E76K-driven juvenile myelomonocytic leukemia. Blood Adv *4*, 3246-3251.

Caiado, F., Kovtonyuk, L.V., Gonullu, N.G., Fullin, J., Boettcher, S., and Manz, M.G. (2023). Aging drives Tet2+/- clonal hematopoiesis via IL-1 signaling. Blood *141*, 886-903.

Caiado, F., Pietras, E.M., and Manz, M.G. (2021). Inflammation as a regulator of hematopoietic stem cell function in disease, aging, and clonal selection. J Exp Med *218*.

Chu, S.H., Heiser, D., Li, L., Kaplan, I., Collector, M., Huso, D., Sharkis, S.J., Civin, C., and Small, D.

(2012). FLT3-ITD knockin impairs hematopoietic stem cell quiescence/homeostasis, leading to myeloproliferative neoplasm. Cell Stem Cell *11*, 346-358.

Cumbo, C., Tarantini, F., Zagaria, A., Anelli, L., Minervini, C.F., Coccaro, N., Tota, G., Impera, L., Parciante, E., Conserva, M.R.*, et al.* (2022). Clonal Hematopoiesis at the Crossroads of Inflammatory Bowel Diseases and Hematological Malignancies: A Biological Link? Front Oncol *12*, 873896.

Delhommeau, F., Dupont, S., Della Valle, V., James, C., Trannoy, S., Massé, A., Kosmider, O., Le Couedic, J.P., Robert, F., Alberdi, A.*, et al.* (2009). Mutation in TET2 in myeloid cancers. N Engl J Med *360*, 2289-2301.

Deshmukh, H.S., Liu, Y., Menkiti, O.R., Mei, J., Dai, N., O'Leary, C.E., Oliver, P.M., Kolls, J.K., Weiser, J.N., and Worthen, G.S. (2014). The microbiota regulates neutrophil homeostasis and host resistance to Escherichia coli K1 sepsis in neonatal mice. Nat Med *20*, 524-530.

Fabre, M.A., de Almeida, J.G., Fiorillo, E., Mitchell, E., Damaskou, A., Rak, J., Orrù, V., Marongiu, M., Chapman, M.S., Vijayabaskar, M.S.*, et al.* (2022). The longitudinal dynamics and natural history of clonal haematopoiesis. Nature *606*, 335-342.

Genovese, G., Kähler, A.K., Handsaker, R.E., Lindberg, J., Rose, S.A., Bakhoum, S.F., Chambert, K., Mick, E., Neale, B.M., Fromer, M.*, et al.* (2014). Clonal hematopoiesis and blood-cancer risk inferred from blood DNA sequence. N Engl J Med *371*, 2477-2487.

He, H., Wang, Z., Yu, H., Zhang, G., Wen, Y., and Cai, Z. (2022). Prioritizing risk genes as novel stratification biomarkers for acute monocytic leukemia by integrative analysis. Discov Oncol *13*, 55.

Heyde, A., Rohde, D., McAlpine, C.S., Zhang, S., Hoyer, F.F., Gerold, J.M., Cheek, D., Iwamoto, Y., Schloss, M.J., Vandoorne, K.*, et al.* (2021). Increased stem cell proliferation in atherosclerosis accelerates clonal hematopoiesis. Cell *184*, 1348-1361.e1322.

Hsu, J.I., Dayaram, T., Tovy, A., De Braekeleer, E., Jeong, M., Wang, F., Zhang, J., Heffernan, T.P., Gera, S., Kovacs, J.J.*, et al.* (2018). PPM1D Mutations Drive Clonal Hematopoiesis in Response to Cytotoxic Chemotherapy. Cell Stem Cell *23*, 700-713.e706.

Jaiswal, S., and Ebert, B.L. (2019). Clonal hematopoiesis in human aging and disease. Science *366*.

Jaiswal, S., and Libby, P. (2020). Clonal haematopoiesis: connecting ageing and inflammation in cardiovascular disease. Nat Rev Cardiol *17*, 137-144.

Jaiswal, S., Natarajan, P., Silver, A.J., Gibson, C.J., Bick, A.G., Shvartz, E., McConkey, M., Gupta, N., Gabriel, S., Ardissino, D.*, et al.* (2017). Clonal Hematopoiesis and Risk of Atherosclerotic Cardiovascular Disease. N Engl J Med *377*, 111-121.

Khan, N., Patel, D., Trivedi, C., Kavani, H., Pernes, T., Medvedeva, E., Lewis, J., Xie, D., and Yang, Y.X. (2021). Incidence of Acute Myeloid Leukemia and Myelodysplastic Syndrome in Patients With Inflammatory Bowel Disease and the Impact of Thiopurines on Their Risk. Am J Gastroenterol *116*, 741-747.

Khoury, J.D., Solary, E., Abla, O., Akkari, Y., Alaggio, R., Apperley, J.F., Bejar, R., Berti, E., Busque, L., Chan, J.K.C.*, et al.* (2022). The 5th edition of the World Health Organization Classification of Haematolymphoid Tumours: Myeloid and Histiocytic/Dendritic Neoplasms. Leukemia *36*, 1703-1719.

La Manno, G., Soldatov, R., Zeisel, A., Braun, E., Hochgerner, H., Petukhov, V., Lidschreiber, K., Kastriti, M.E., Lönnerberg, P., Furlan, A.*, et al.* (2018). RNA velocity of single cells. Nature *560*, 494-498.

Li, S., Zhang, P., Chen, W., Ye, L., Brannan, K.W., Le, N.-T., Abe, J.-i., Cooke, J.P., and Wang, G. (2023). A relay velocity model infers cell-dependent RNA velocity. Nature Biotechnology.

Libby, P., Ridker, P.M., and Maseri, A. (2002). Inflammation and atherosclerosis. Circulation *105*, 1135-1143.

Meisel, M., Hinterleitner, R., Pacis, A., Chen, L., Earley, Z.M., Mayassi, T., Pierre, J.F., Ernest, J.D., Galipeau, H.J., Thuille, N., *et al.* (2018). Microbial signals drive pre-leukaemic myeloproliferation in a Tet2-deficient host. Nature *557*, 580-584.

Miller, P.G., Qiao, D., Rojas-Quintero, J., Honigberg, M.C., Sperling, A.S., Gibson, C.J., Bick, A.G., Niroula, A., McConkey, M.E., Sandoval, B., *et al.* (2022). Association of clonal hematopoiesis with chronic obstructive pulmonary disease. Blood *139*, 357-368.

Moran-Crusio, K., Reavie, L., Shih, A., Abdel-Wahab, O., Ndiaye-Lobry, D., Lobry, C., Figueroa, M.E., Vasanthakumar, A., Patel, J., Zhao, X., *et al.* (2011). Tet2 loss leads to increased hematopoietic stem cell self-renewal and myeloid transformation. Cancer Cell *20*, 11-24.

Nazha, A., Komrokji, R., Meggendorfer, M., Jia, X., Radakovich, N., Shreve, J., Hilton, C.B., Nagata, Y., Hamilton, B.K., Mukherjee, S., *et al.* (2021). Personalized Prediction Model to Risk Stratify Patients With Myelodysplastic Syndromes. J Clin Oncol *39*, 3737-3746.

Rasmussen, K.D., Jia, G., Johansen, J.V., Pedersen, M.T., Rapin, N., Bagger, F.O., Porse, B.T., Bernard, O.A., Christensen, J., and Helin, K. (2015). Loss of TET2 in hematopoietic cells leads to DNA hypermethylation of active enhancers and induction of leukemogenesis. Genes Dev *29*, 910-922.

Smillie, C.S., Biton, M., Ordovas-Montanes, J., Sullivan, K.M., Burgin, G., Graham, D.B., Herbst, R.H., Rogel, N., Slyper, M., Waldman, J., *et al.* (2019). Intra- and Inter-cellular Rewiring of the Human Colon during Ulcerative Colitis. Cell *178*, 714-730.e722.

Steensma, D.P., Bejar, R., Jaiswal, S., Lindsley, R.C., Sekeres, M.A., Hasserjian, R.P., and Ebert, B.L. (2015). Clonal hematopoiesis of indeterminate potential and its distinction from myelodysplastic syndromes. Blood *126*, 9-16.

Taur, Y., Xavier, J.B., Lipuma, L., Ubeda, C., Goldberg, J., Gobourne, A., Lee, Y.J., Dubin, K.A., Socci, N.D., Viale, A., *et al.* (2012). Intestinal domination and the risk of bacteremia in patients undergoing allogeneic hematopoietic stem cell transplantation. Clin Infect Dis *55*, 905-914.

Weeks, L.D., Niroula, A., Neuberg, D.S., Wong, W.J., Lindsley, R.C., Luskin, M.R., Berliner, N., Stone, R.M., DeAngelo, D.J., Soiffer, R.J., *et al.* (2022). Prediction of Risk for Myeloid Malignancy in Clonal Hematopoiesis. Blood *140*, 2229-2231.

Weinstock, J.S., Gopakumar, J., Burugula, B.B., Uddin, M.M., Jahn, N., Belk, J.A., Bouzid, H., Daniel, B., Miao, Z., Ly, N., *et al.* (2023). Aberrant activation of TCL1A promotes stem cell expansion in clonal haematopoiesis. Nature *616*, 755-763.

Wong, T.N., Ramsingh, G., Young, A.L., Miller, C.A., Touma, W., Welch, J.S., Lamprecht, T.L., Shen, D., Hundal, J., Fulton, R.S., *et al.* (2015). Role of TP53 mutations in the origin and evolution of therapy-related acute myeloid leukaemia. Nature *518*, 552-555.

Yan, H., Baldridge, M.T., and King, K.Y. (2018). Hematopoiesis and the bacterial microbiome. Blood *132*, 559-564.

Zeng, H., He, H., Guo, L., Li, J., Lee, M., Han, W., Guzman, A.G., Zang, S., Zhou, Y., Zhang, X., *et al.* (2019). Antibiotic treatment ameliorates Ten-eleven translocation 2 (TET2) loss-of-function associated hematological malignancies. Cancer Lett *467*, 1-8.

Zeng, X., Li, X., Li, X., Wei, C., Shi, C., Hu, K., Kong, D., Luo, Q., Xu, Y., Shan, W., *et al.* (2023). Fecal microbiota transplantation from young mice rejuvenates aged hematopoietic stem cells by suppressing inflammation. Blood *141*, 1691-1707.

Zhang, C.R.C., Nix, D., Gregory, M., Ciorba, M.A., Ostrander, E.L., Newberry, R.D., Spencer, D.H., and Challen, G.A. (2019). Inflammatory cytokines promote clonal hematopoiesis with specific mutations in ulcerative colitis patients. Exp Hematol *80*, 36-41.e33.

Zhang, Q., Zhao, K., Shen, Q., Han, Y., Gu, Y., Li, X., Zhao, D., Liu, Y., Wang, C., Zhang, X.*, et al.* (2015). Tet2 is required to resolve inflammation by recruiting Hdac2 to specifically repress IL-6. Nature *525*, 389-393.

Figure 1.

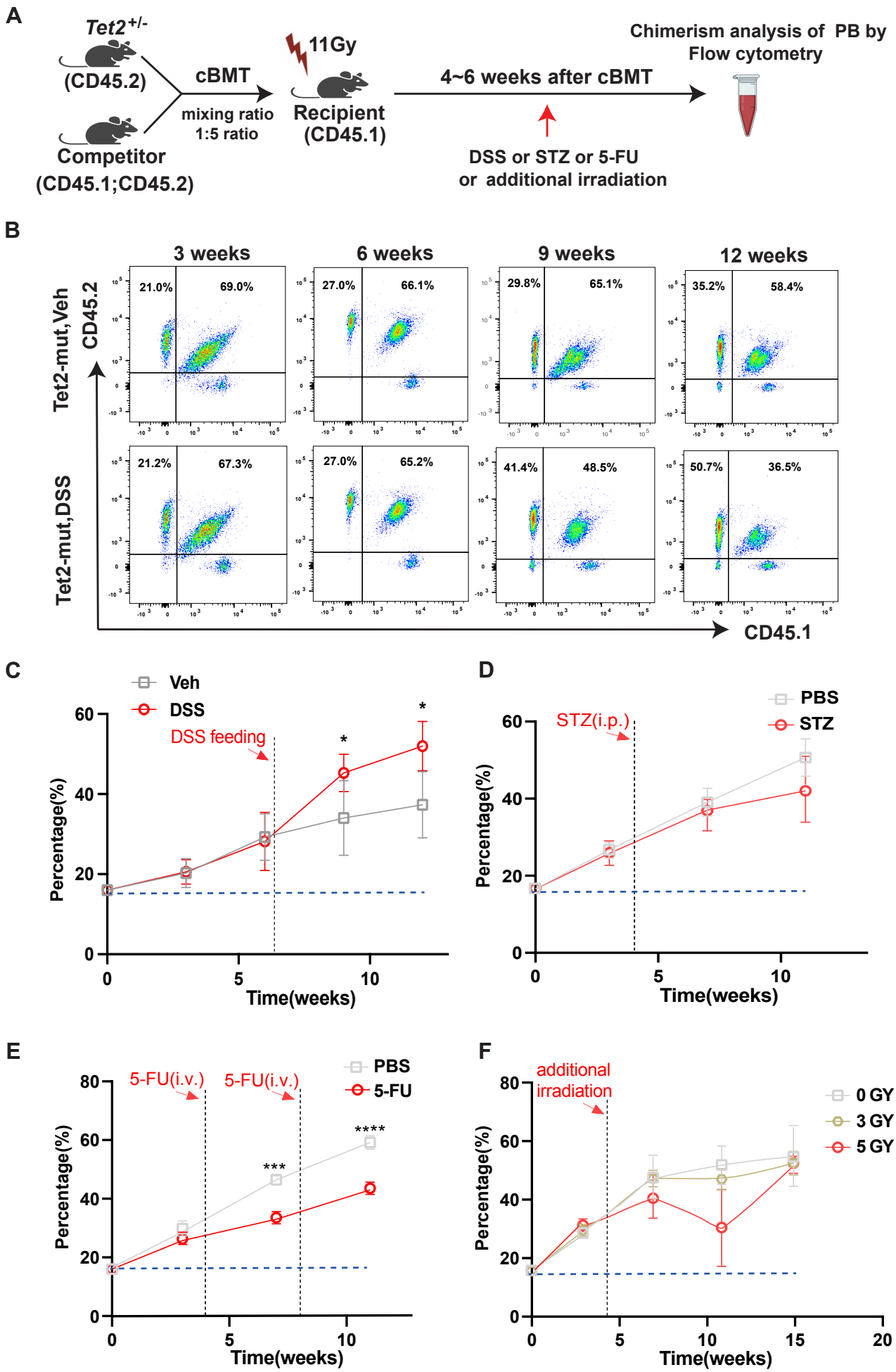
A
Tet2+/-
(CD45.2)
Competitor
(CD45.1;CD45.2)
cBMT
mixing ratio
1:5 ratio
11Gy
Recipient
(CD45.1)
4~6 weeks after cBMT
DSS or STZ or 5-FU
or additional irradiation
Chimerism analysis of PB by
Flow cytometry
B
3 weeks
6 weeks
9 weeks
12 weeks
Tet2-mut,Veh
Tet2-mut,DSS
CD45.2
CD45.1
21.0%
69.0%
27.0%
66.1%
29.8%
65.1%
35.2%
58.4%
21.2%
67.3%
27.0%
65.2%
41.4%
48.5%
50.7%
36.5%
C
Veh
DSS
DSS feeding
Percentage(%)
Time(weeks)
D
PBS
STZ
STZ(i.p.)
Percentage(%)
Time(weeks)
E
PBS
5-FU
5-FU(i.v.)
5-FU(i.v.)
Percentage(%)
Time(weeks)
F
0 GY
3 GY
5 GY
additional
irradiation
Percentage(%)
Time(weeks)

Figure 2.

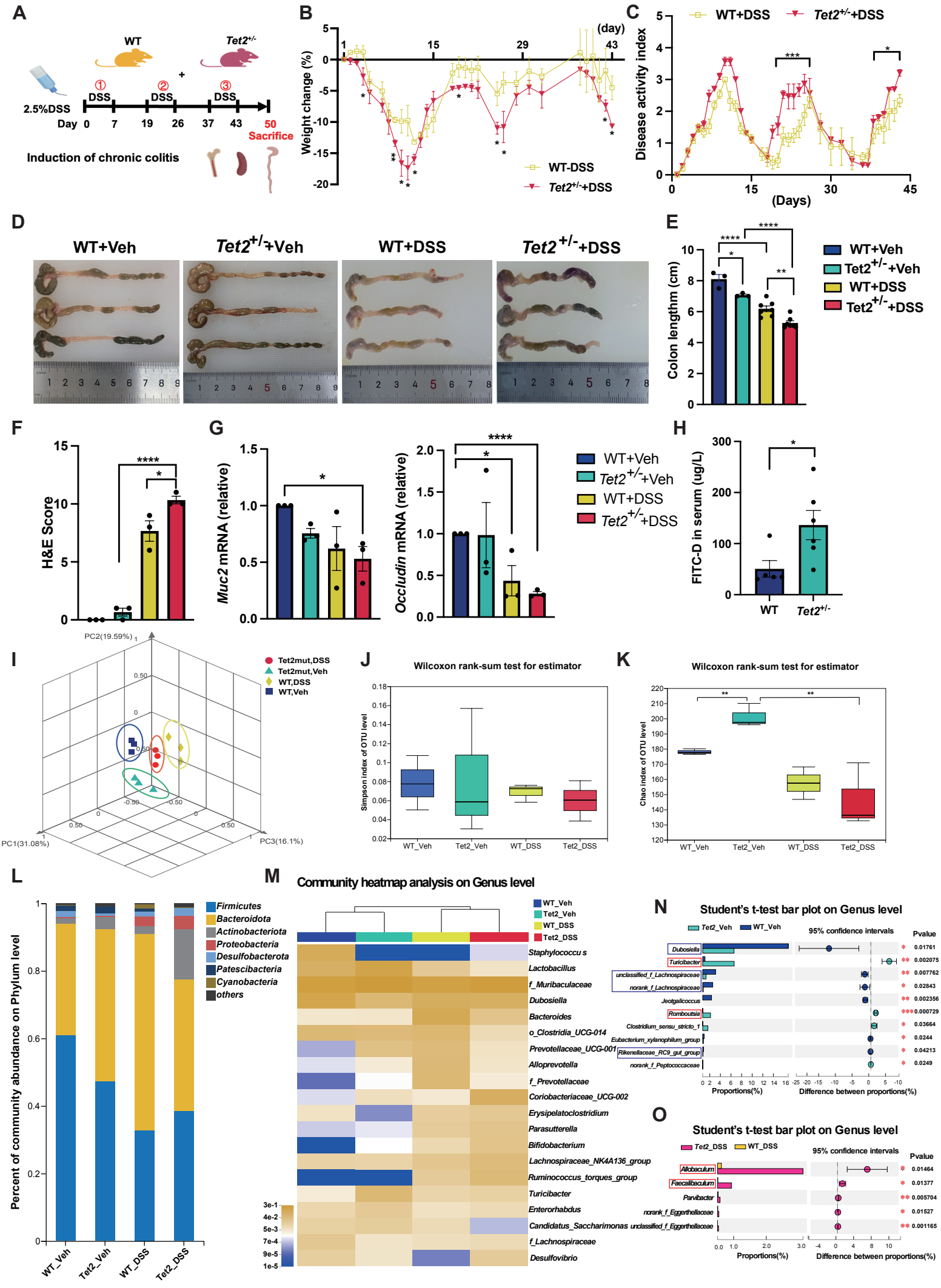
A
WT
Tet2+/-
2.5%DSS
① DSS
② DSS
③ DSS
Day 0 7 19 26 37 43 50
Sacrifice
Induction of chronic colitis
B
Weight change (%)
(day)
WT-DSS
Tet2+/-+DSS
C
WT+DSS
Tet2+/-+DSS
Disease activity index
(Days)
D
WT+Veh
Tet2+/-+Veh
WT+DSS
Tet2+/-+DSS
E
Colon lengthm (cm)
WT+Veh
Tet2+/-+Veh
WT+DSS
Tet2+/-+DSS
F
H&E Score
G
Muc2 mRNA (relative)
Occludin mRNA (relative)
WT+Veh
Tet2+/-+Veh
WT+DSS
Tet2+/-+DSS
H
FITC-D in serum (ug/L)
WT
Tet2+/-
I
PC2(19.59%)
PC1(31.08%)
PC3(16.1%)
Tet2mut,DSS
Tet2mut,Veh
WT,DSS
WT,Veh
J
Wilcoxon rank-sum test for estimator
Simpson index of OTU level
WT_Veh
Tet2_Veh
WT_DSS
Tet2_DSS
K
Wilcoxon rank-sum test for estimator
Chao index of OTU level
WT_Veh
Tet2_Veh
WT_DSS
Tet2_DSS
L
Percent of community abundance on Phylum level
Firmicutes
Bacteroidota
Actinobacteriota
Proteobacteria
Desulfobacterota
Patescibacteria
Cyanobacteria
others
WT_Veh
Tet2_Veh
WT_DSS
Tet2_DSS
M
Community heatmap analysis on Genus level
WT_Veh
Tet2_Veh
WT_DSS
Tet2_DSS
Staphylococcus
Lactobacillus
f_Muribaculaceae
Dubosiella
Bacteroides
o_Clostridia_UCG-014
Prevotellaceae_UCG-001
Alloprevotella
f_Prevotellaceae
Coriobacteriaceae_UCG-002
Erysipelatoclostridium
Parasutterella
Bifidobacterium
Lachnospiraceae_NK4A136_group
Ruminococcus_torques_group
Turicibacter
Enterorhabdus
Candidatus_Saccharimonas
f_Lachnospiraceae
Desulfovibrio
N
Student's t-test bar plot on Genus level
Tet2_Veh
WT_Veh
95% confidence intervals
Pvalue
Dubosiella
Turicibacter
unclassified_f_Lachnospiraceae
norank_f_Lachnospiraceae
Jeotgalicoccus
Romboutsia
Clostridium_sensu_stricto_1
Eubacterium_xylanophilum_group
Rikenellaceae_RC9_gut_group
norank_f_Peptococcaceae
Proportions(%)
Difference between proportions(%)
O
Student's t-test bar plot on Genus level
Tet2_DSS
WT_DSS
95% confidence intervals
Pvalue
Allobaculum
Faecalibaculum
Parvibacter
norank_f_Eggerthellaceae
unclassified_f_Eggerthellaceae
Proportions(%)
Difference between proportions(%)

Figure 3.

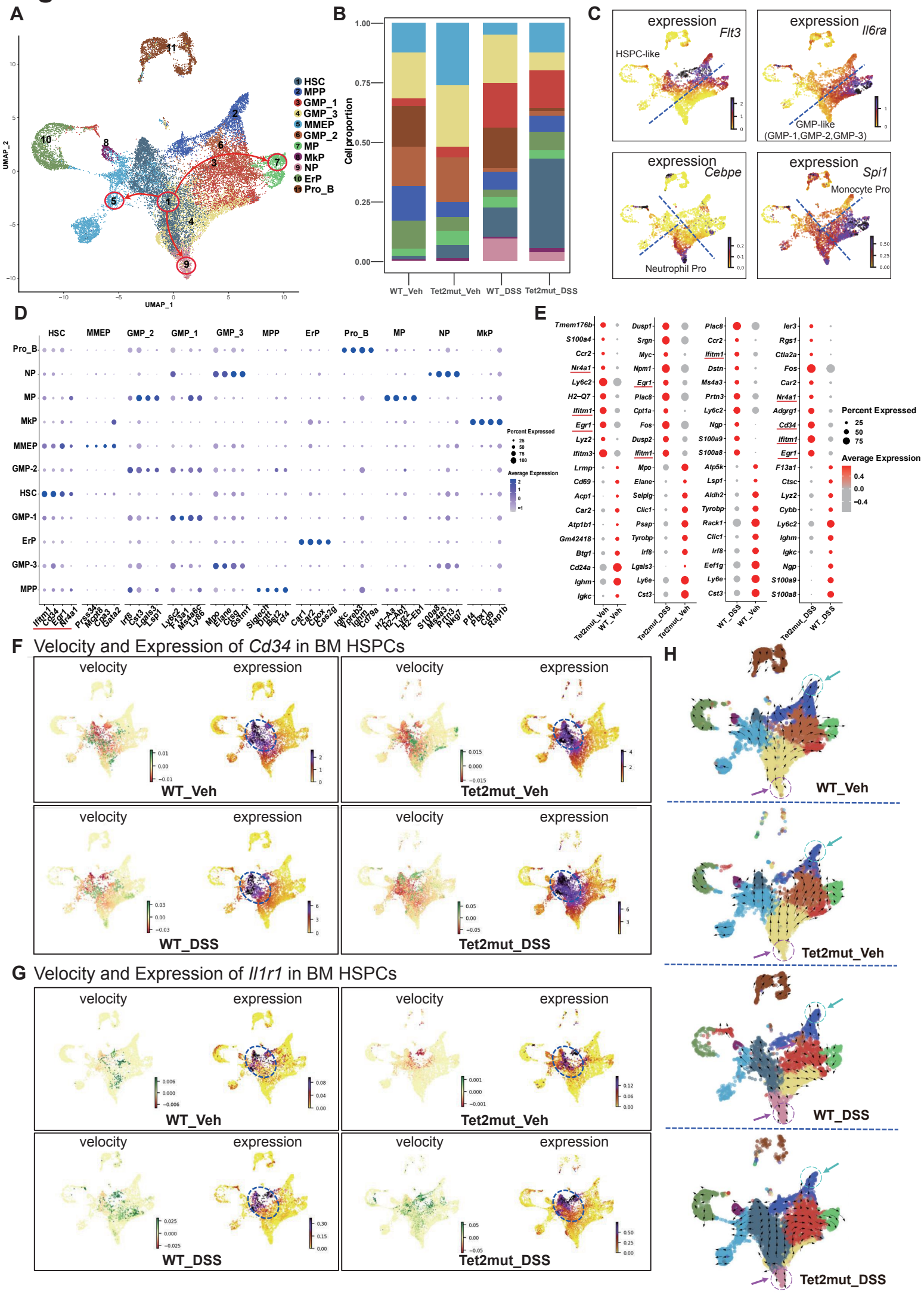
A
UMAP_1
UMAP_2
1 HSC
2 MPP
3 GMP_1
4 GMP_3
5 MMEP
6 GMP_2
7 MP
8 MkP
9 NP
10 ErP
11 Pro_B
B
Cell proportion
WT_Veh
Tet2mut_Veh
WT_DSS
Tet2mut_DSS
C
expression Flt3
HSPC-like
expression Il6ra
GMP-like (GMP-1,GMP-2,GMP-3)
expression Cebpe
Neutrophil Pro
expression Spi1
Monocyte Pro
D
HSC
MMEP
GMP_2
GMP_1
GMP_3
MPP
ErP
Pro_B
MP
NP
MkP
Percent Expressed
Average Expression
E
Percent Expressed
Average Expression
F Velocity and Expression of Cd34 in BM HSPCs
velocity
expression
WT_Veh
Tet2mut_Veh
WT_DSS
Tet2mut_DSS
G Velocity and Expression of Il1r1 in BM HSPCs
velocity
expression
WT_Veh
Tet2mut_Veh
WT_DSS
Tet2mut_DSS
H
WT_Veh
Tet2mut_Veh
WT_DSS
Tet2mut_DSS

Figure 4.

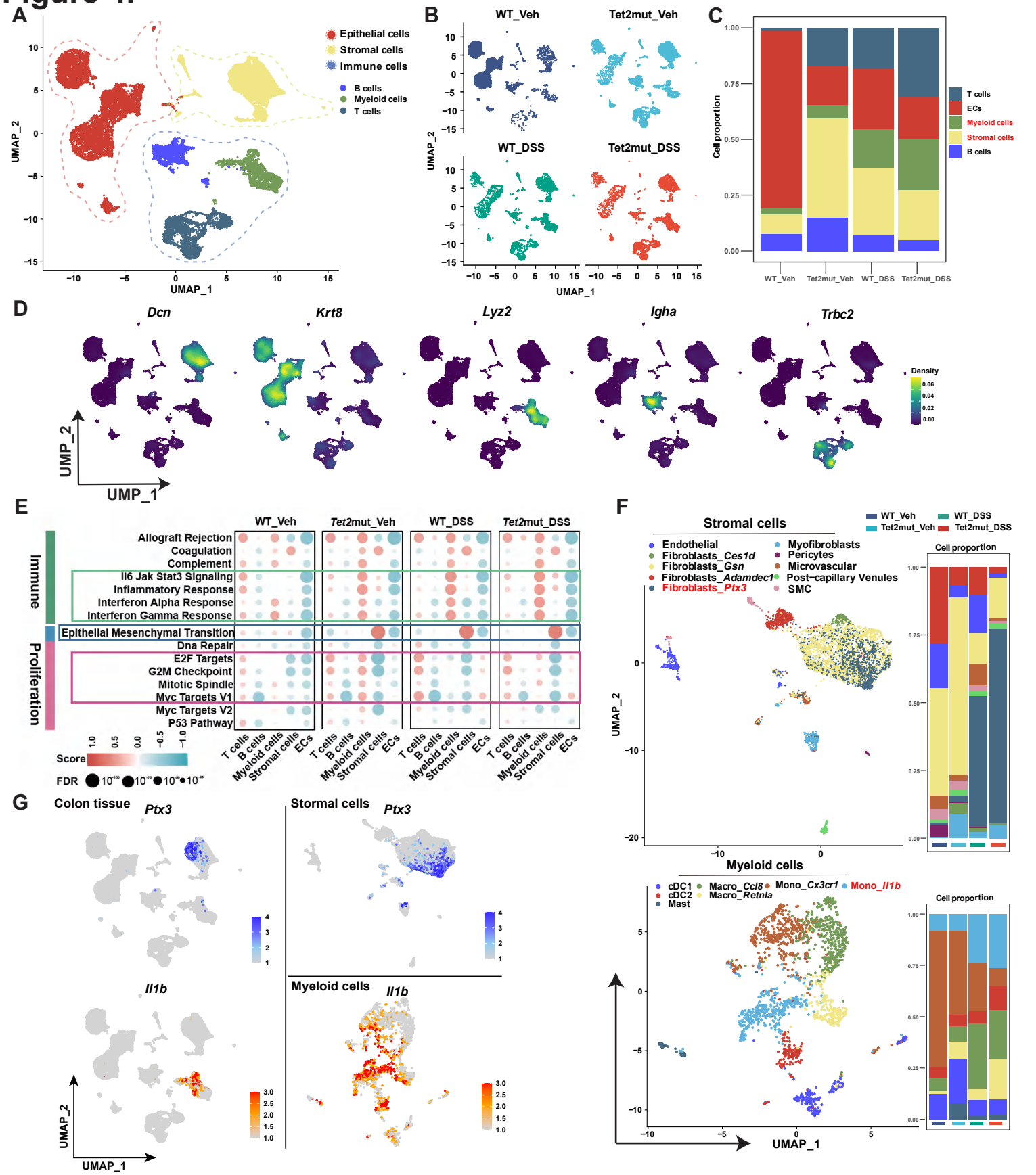
A
Epithelial cells
Stromal cells
Immune cells
B cells
Myeloid cells
T cells
UMAP_1
UMAP_2
B
WT_Veh
Tet2mut_Veh
WT_DSS
Tet2mut_DSS
C
Cell proportion
T cells
ECs
Myeloid cells
Stromal cells
B cells
D
Dcn
Krt8
Lyz2
Igha
Trbc2
Density
E
WT_Veh
Tet2mut_Veh
WT_DSS
Tet2mut_DSS
Immune
Proliferation
Allograft Rejection
Coagulation
Complement
Il6 Jak Stat3 Signaling
Inflammatory Response
Interferon Alpha Response
Interferon Gamma Response
Epithelial Mesenchymal Transition
Dna Repair
E2F Targets
G2M Checkpoint
Mitotic Spindle
Myc Targets V1
Myc Targets V2
P53 Pathway
Score
FDR
F
Stromal cells
Endothelial
Fibroblasts_Ces1d
Fibroblasts_Gsn
Fibroblasts_Adamdec1
Fibroblasts_Ptx3
Myofibroblasts
Pericytes
Microvascular
Post-capillary Venules
SMC
Cell proportion
Myeloid cells
cDC1
cDC2
Mast
Macro_Ccl8
Macro_Retnla
Mono_Cx3cr1
Mono_Il1b
G
Colon tissue
Ptx3
Stormal cells
Il1b
Myeloid cells
H
WT_Veh
Tet2mut_Veh
WT_DSS
Tet2mut_DSS
Interaction strength

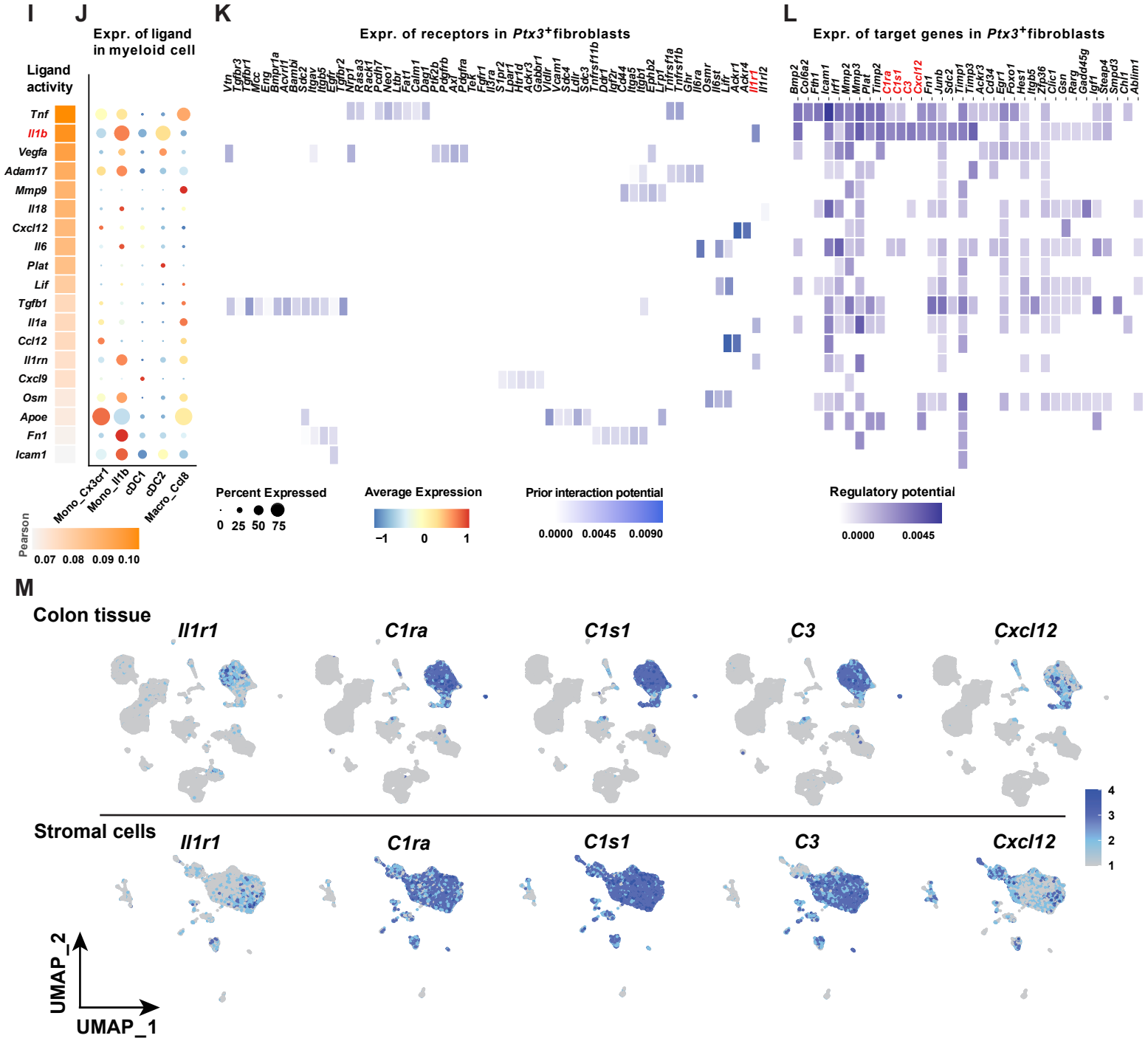
I
J
Expr. of ligand in myeloid cell
Ligand activity
Tnf
Il1b
Vegfa
Adam17
Mmp9
Il18
Cxcl12
Il6
Plat
Lif
Tgfb1
Il1a
Ccl12
Il1rn
Cxcl9
Osm
Apoe
Fn1
Icam1
Mono_Cx3cr1
Mono_Il1b
cDC1
cDC2
Macro_Ccl8
Pearson
0.07 0.08 0.09 0.10
K
Expr. of receptors in Ptx3+fibroblasts
Percent Expressed
0 25 50 75
Average Expression
−1 0 1
Prior interaction potential
0.0000 0.0045 0.0090
L
Expr. of target genes in Ptx3+fibroblasts
Regulatory potential
0.0000 0.0045
M
Colon tissue
Il1r1
C1ra
C1s1
C3
Cxcl12
Stromal cells
Il1r1
C1ra
C1s1
C3
Cxcl12
4
3
2
1
UMAP_2
UMAP_1

Figure 5.

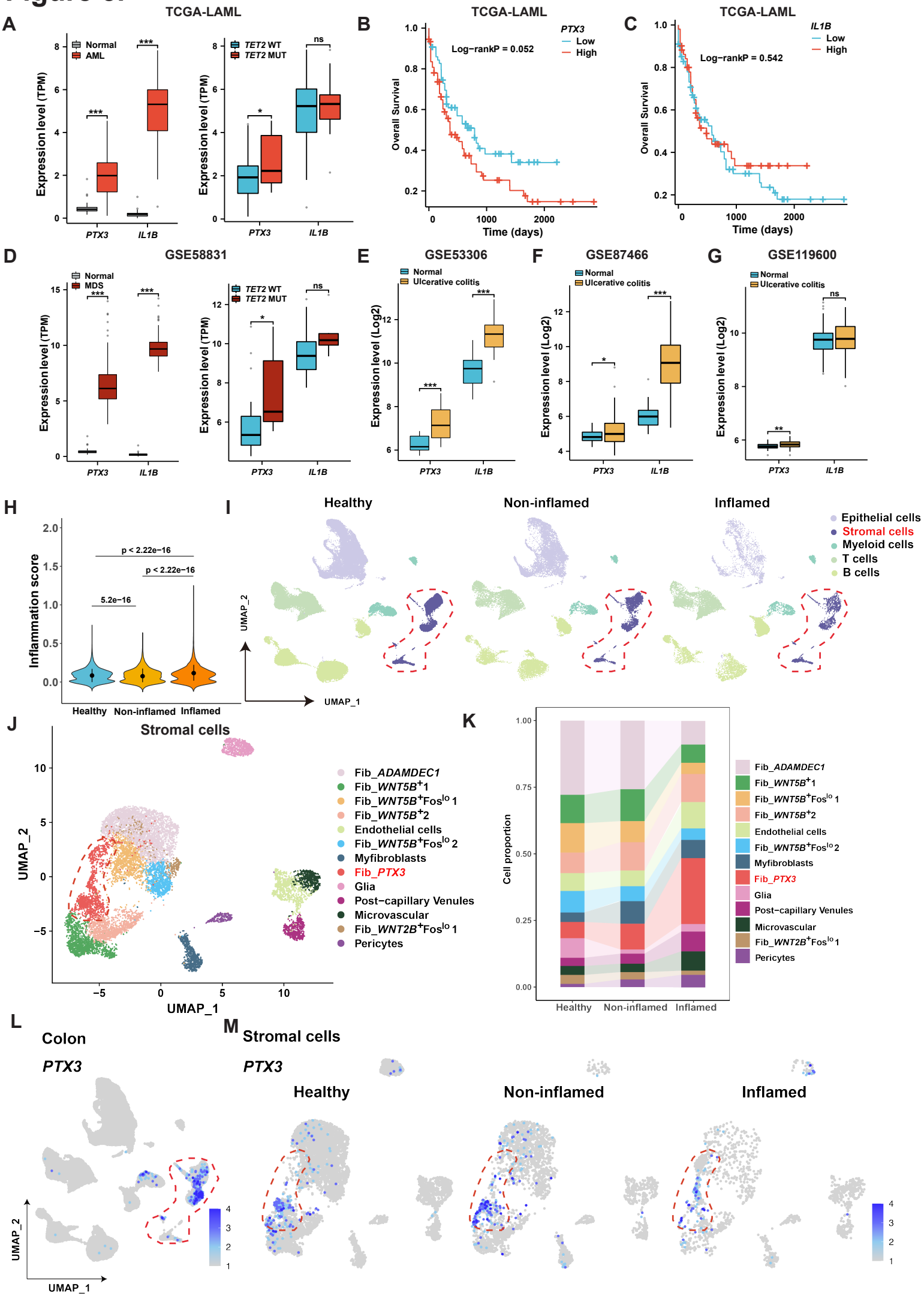
A
TCGA-LAML
Normal
AML
Expression level (TPM)
PTX3
IL1B
TET2 WT
TET2 MUT
B
TCGA-LAML
PTX3
Low
High
Log−rankP = 0.052
Overall Survival
Time (days)
C
TCGA-LAML
IL1B
Low
High
Log−rankP = 0.542
D
GSE58831
Normal
MDS
E
GSE53306
Normal
Ulcerative colitis
Expression level (Log2)
F
GSE87466
G
GSE119600
H
Inflammation score
p < 2.22e−16
5.2e−16
Healthy
Non-inflamed
Inflamed
I
Healthy
Non-inflamed
Inflamed
Epithelial cells
Stromal cells
Myeloid cells
T cells
B cells
UMAP_1
UMAP_2
J
Stromal cells
Fib_ADAMDEC1
Fib_WNT5B+1
Fib_WNT5B+Fos lo 1
Fib_WNT5B+2
Endothelial cells
Fib_WNT5B+Fos lo 2
Myfibroblasts
Fib_PTX3
Glia
Post−capillary Venules
Microvascular
Fib_WNT2B+Fos lo 1
Pericytes
K
Cell proportion
L
Colon
PTX3
M
Stromal cells
PTX3
Healthy
Non-inflamed
Inflamed

Figure 6

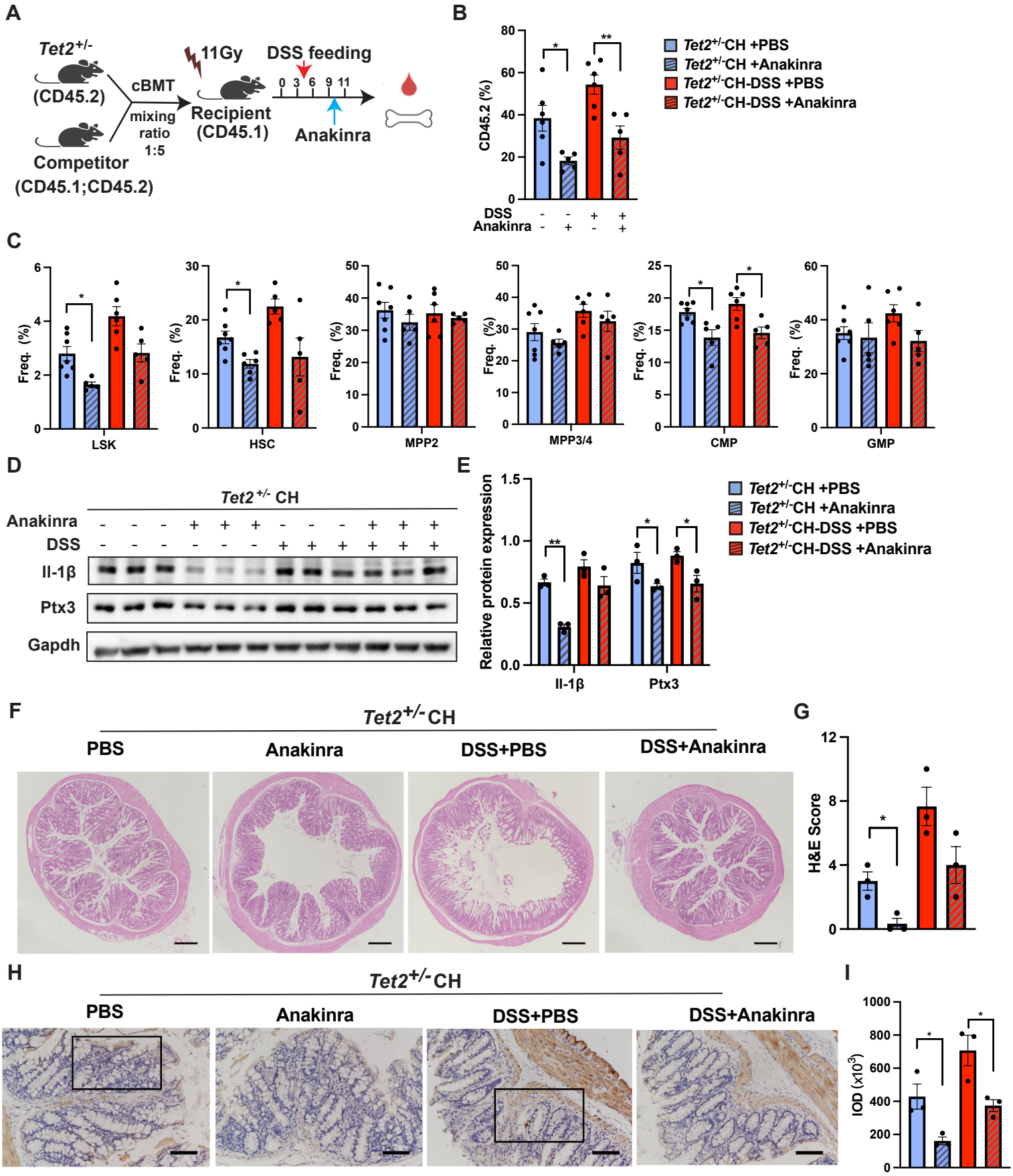
A
Tet2+/-
(CD45.2)
Competitor
(CD45.1;CD45.2)
cBMT
mixing ratio 1:5
11Gy
Recipient (CD45.1)
DSS feeding
0 3 6 9 11
Anakinra
B
CD45.2 (%)
DSS
Anakinra
Tet2+/-CH +PBS
Tet2+/-CH +Anakinra
Tet2+/-CH-DSS +PBS
Tet2+/-CH-DSS +Anakinra
C
Freq. (%)
LSK
HSC
MPP2
MPP3/4
CMP
GMP
D
Tet2+/- CH
Anakinra
DSS
Il-1β
Ptx3
Gapdh
E
Relative protein expression
Il-1β
Ptx3
F
Tet2+/-CH
PBS
Anakinra
DSS+PBS
DSS+Anakinra
G
H&E Score
H
Tet2+/-CH
PBS
Anakinra
DSS+PBS
DSS+Anakinra
I
IOD (x10³)

Figure 7.

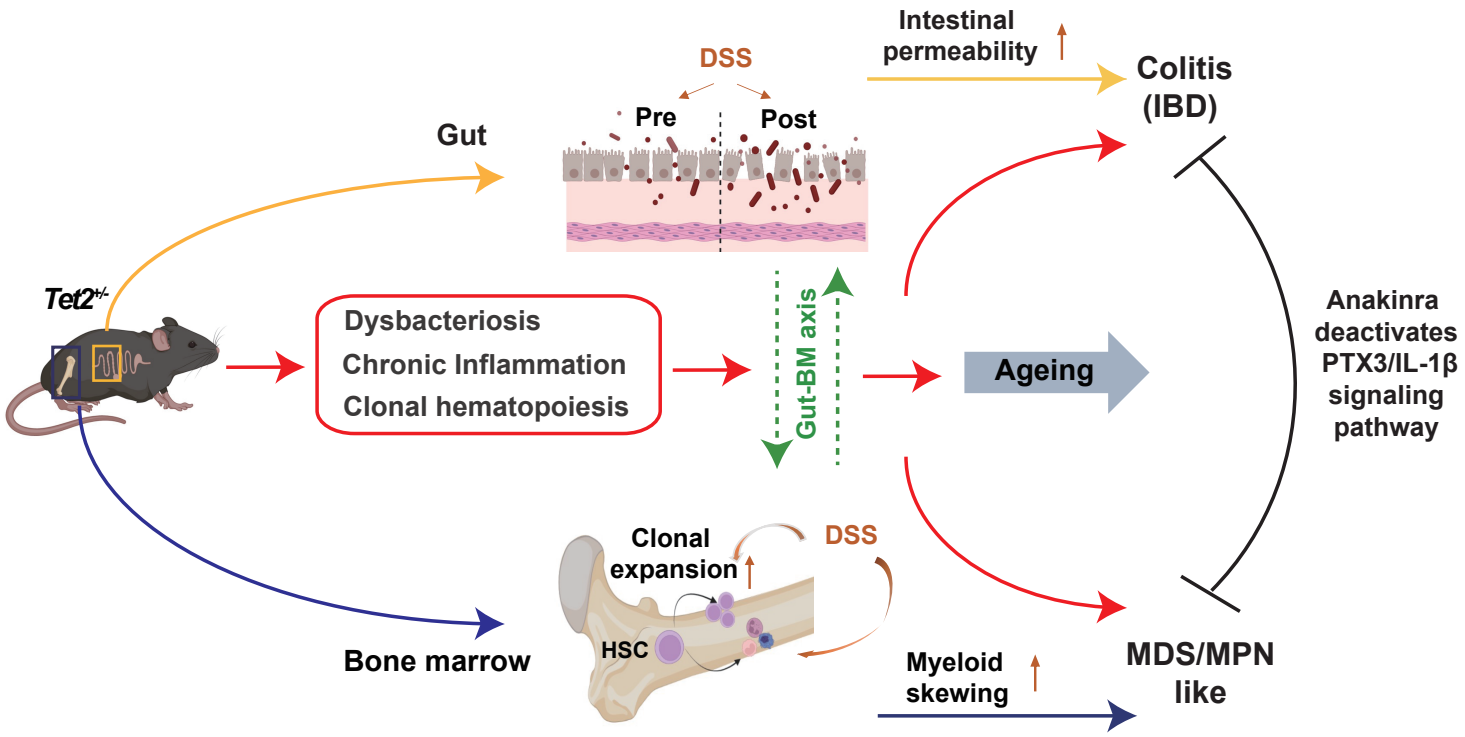
Intestinal permeability
DSS
Colitis (IBD)
Pre
Post
Gut
Tet2+/-
Dysbacteriosis
Chronic Inflammation
Clonal hematopoiesis
Gut-BM axis
Ageing
Anakinra deactivates PTX3/IL-1β signaling pathway
Clonal expansion
DSS
HSC
Bone marrow
Myeloid skewing
MDS/MPN like

Supplemental Figure 1

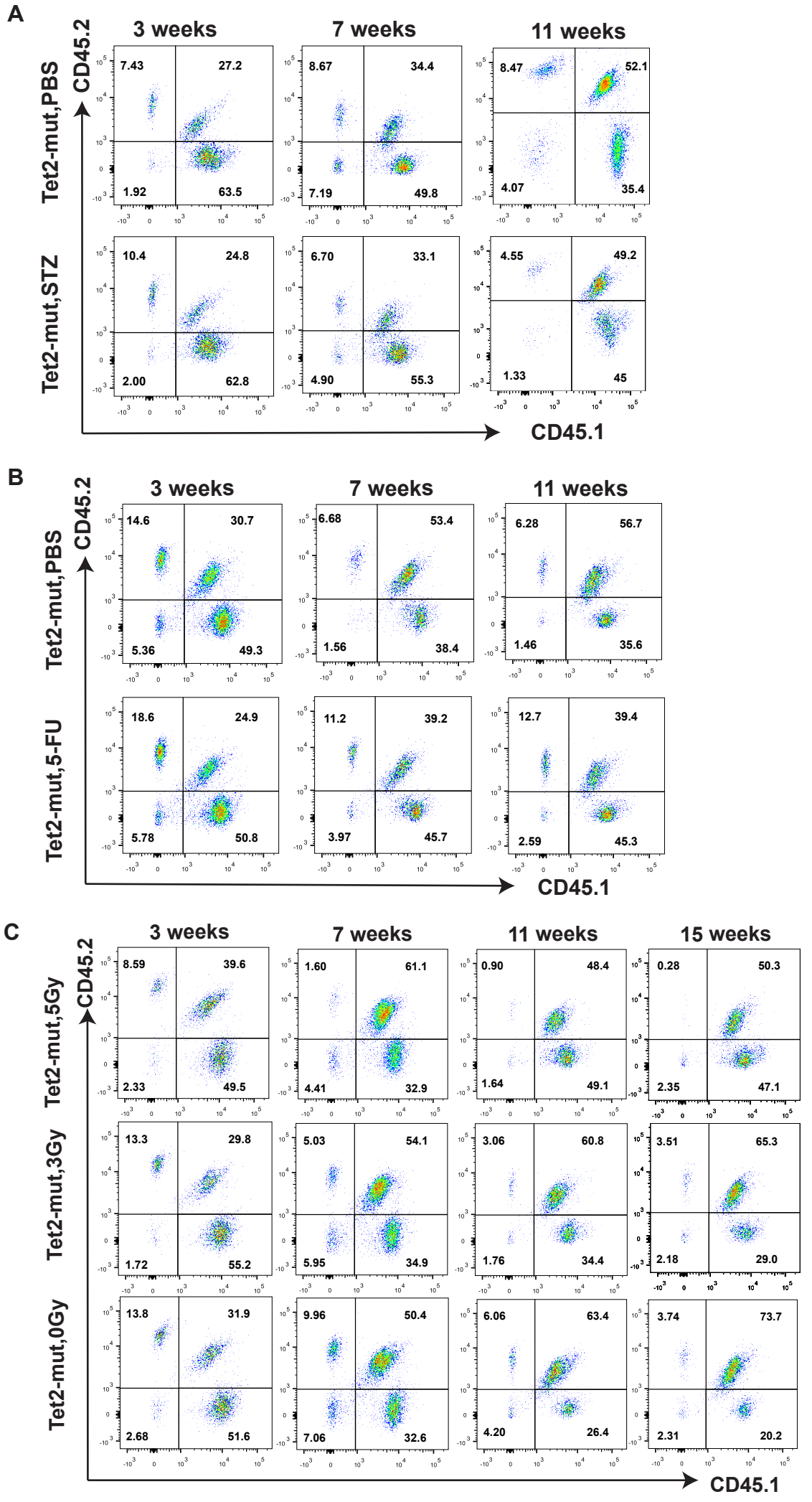

Supplementary Figure 2

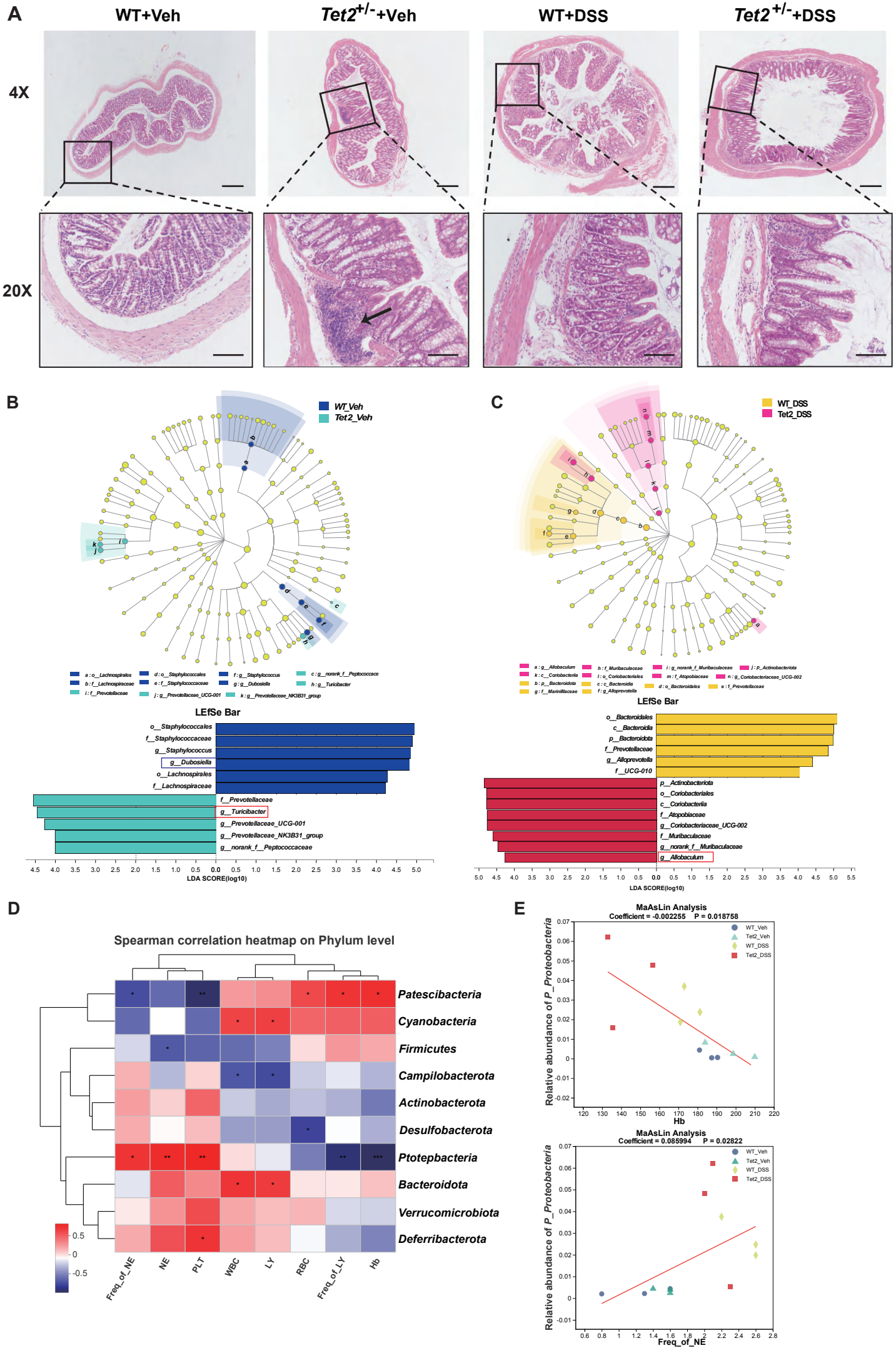

Supplemental Figure 3

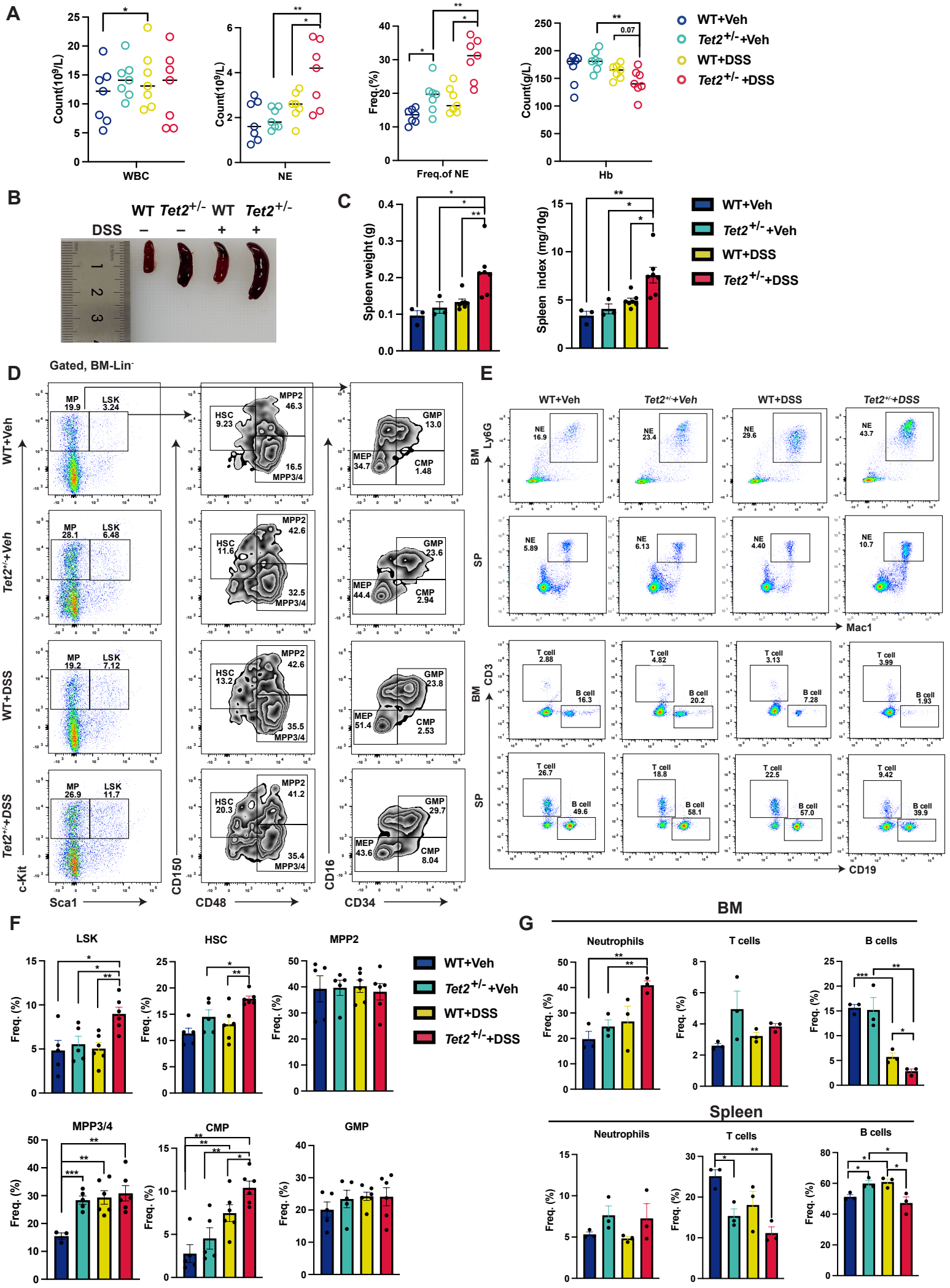

Supplemental Figure 4

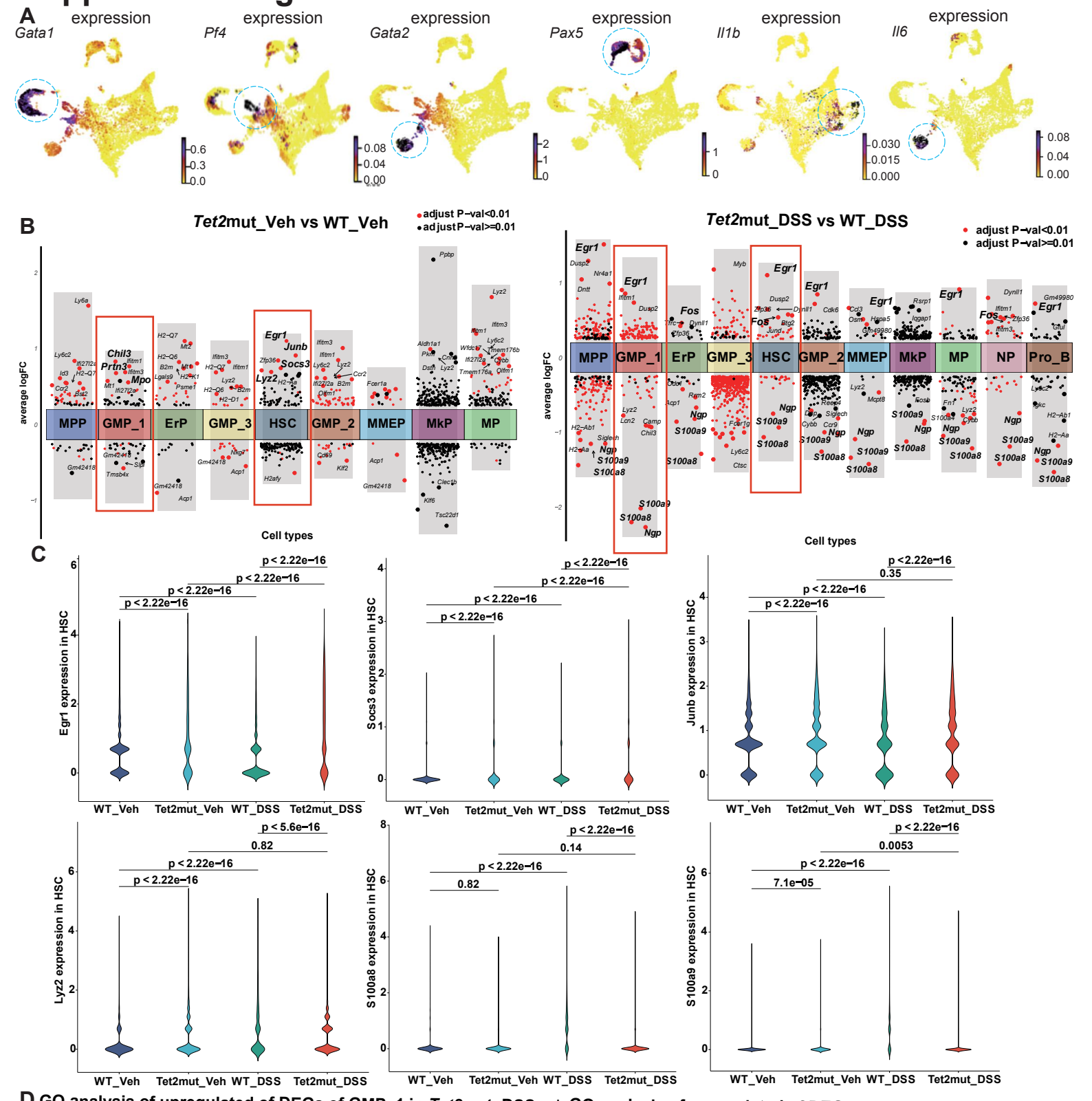

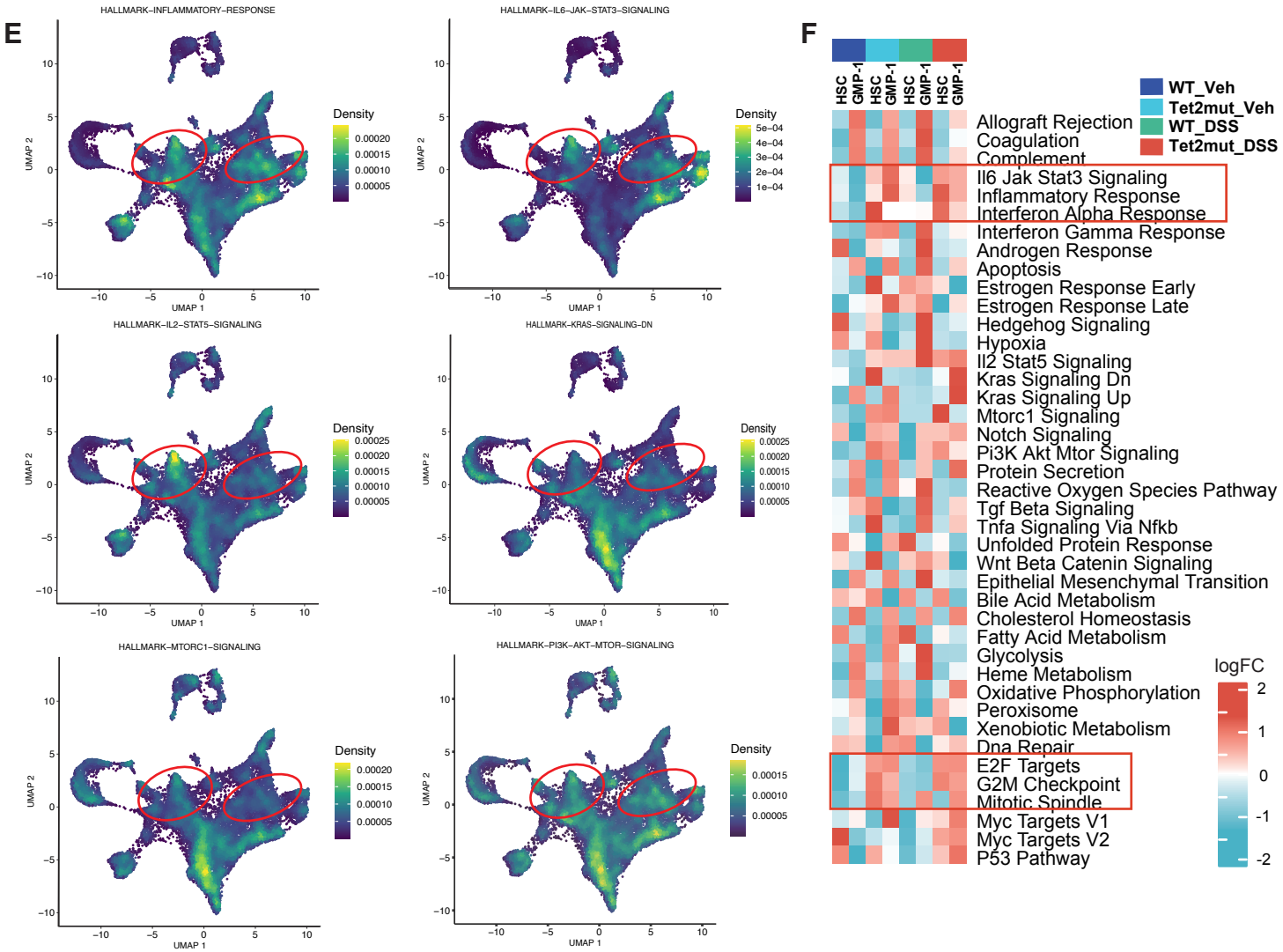
E
HALLMARK-INFLAMMATORY-RESPONSE
HALLMARK-IL6-JAK-STAT3-SIGNALING
HALLMARK-IL2-STAT5-SIGNALING
HALLMARK-KRAS-SIGNALING-DN
HALLMARK-MTORC1-SIGNALING
HALLMARK-PI3K-AKT-MTOR-SIGNALING
Density
UMAP 1
UMAP 2
F
HSC
GMP-1
WT_Veh
Tet2mut_Veh
WT_DSS
Tet2mut_DSS
Allograft Rejection
Coagulation
Complement
Il6 Jak Stat3 Signaling
Inflammatory Response
Interferon Alpha Response
Interferon Gamma Response
Androgen Response
Apoptosis
Estrogen Response Early
Estrogen Response Late
Hedgehog Signaling
Hypoxia
Il2 Stat5 Signaling
Kras Signaling Dn
Kras Signaling Up
Mtorc1 Signaling
Notch Signaling
Pi3K Akt Mtor Signaling
Protein Secretion
Reactive Oxygen Species Pathway
Tgf Beta Signaling
Tnfa Signaling Via Nfkb
Unfolded Protein Response
Wnt Beta Catenin Signaling
Epithelial Mesenchymal Transition
Bile Acid Metabolism
Cholesterol Homeostasis
Fatty Acid Metabolism
Glycolysis
Heme Metabolism
Oxidative Phosphorylation
Peroxisome
Xenobiotic Metabolism
Dna Repair
E2F Targets
G2M Checkpoint
Mitotic Spindle
Myc Targets V1
Myc Targets V2
P53 Pathway
logFC
G
WT_Veh
Tet2mut_Veh
WT_DSS
Tet2mut_DSS

Supplemental Figure 5

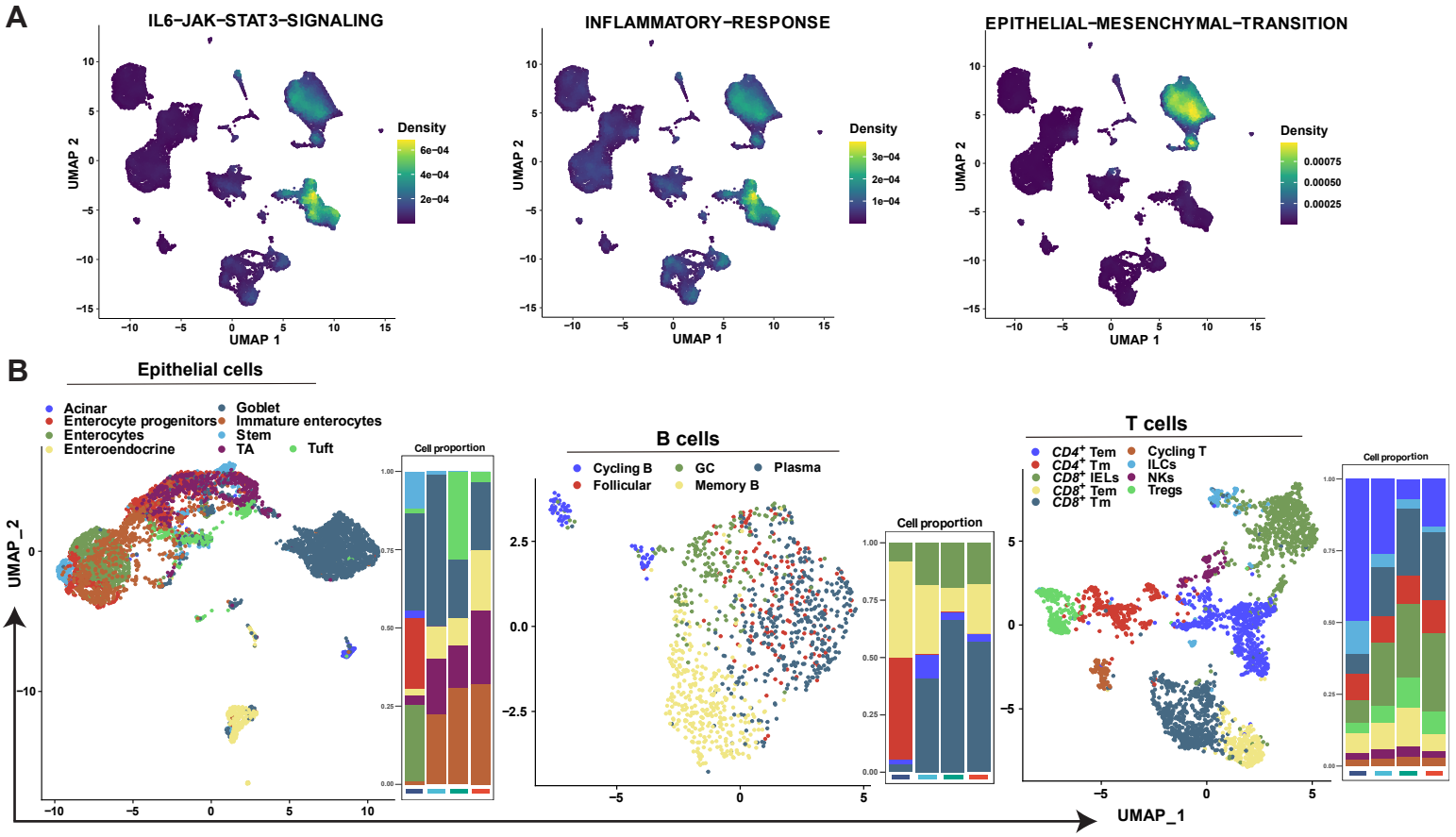

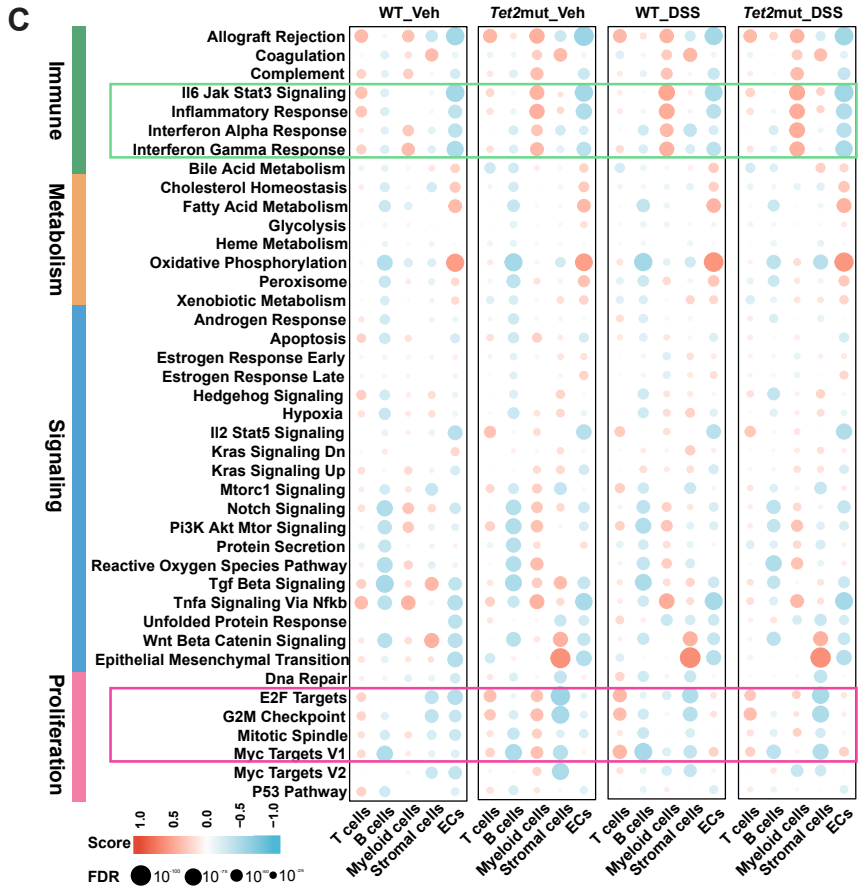

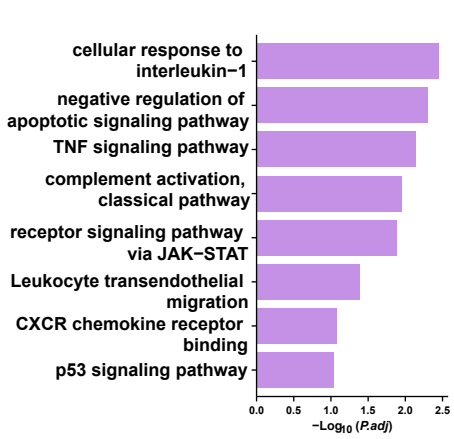

Supplementary Figure 6

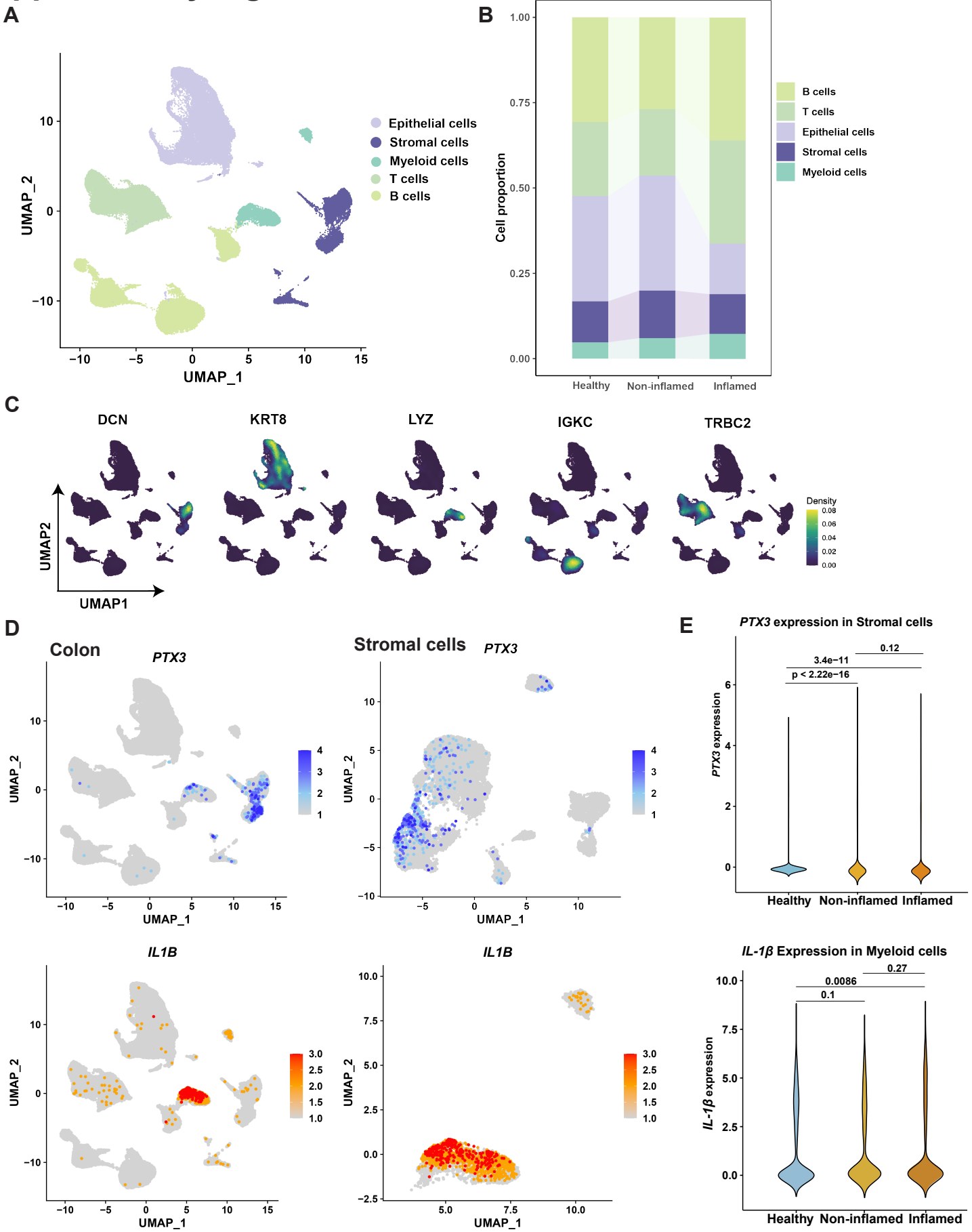
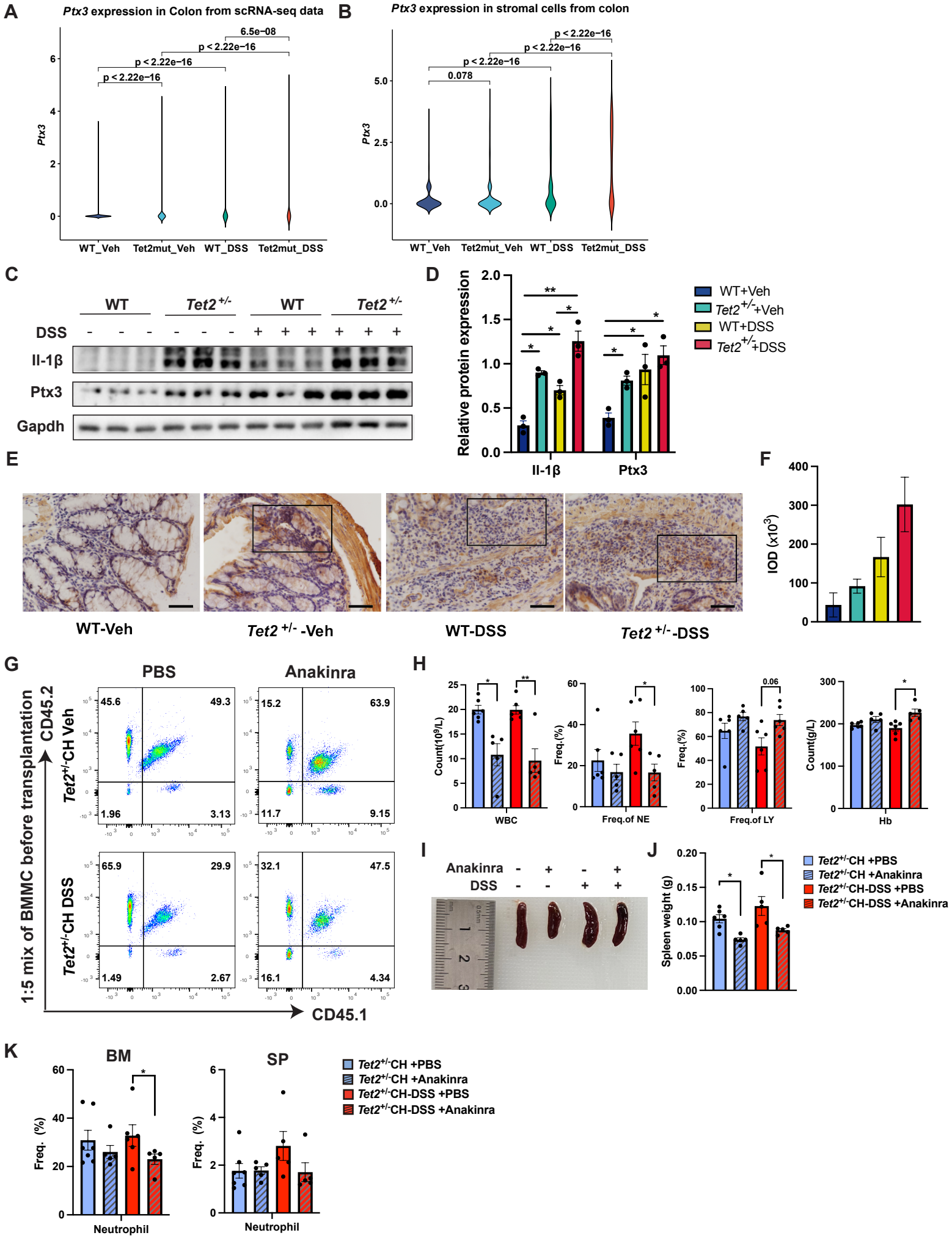
Supplementary Figure 7